DETERMINING ETHANOL CONCENTRATION IN WET DEPOSITION IN THE EASTERN UNITED STATES AND SOUTH TEXAS

A Thesis

by

BIPIN SHARMA

BS, Kathmandu University, 2015

Submitted in Partial Fulfillment of the Requirements for the Degree of

MASTER OF SCIENCE

in

ENVIRONMENTAL SCIENCE

Texas A&M University-Corpus Christi
Corpus Christi, Texas

December 2019

December 2019

DETERMINING ETHANOL CONCENTRATION IN WET DEPOSITION IN THE EASTERN UNITED STATES AND SOUTH TEXAS

A Thesis

by

BIPIN SHARMA

This thesis meets the standards for scope and quality of
Texas A&M University-Corpus Christi and is hereby approved.

Dr. J. D. Felix, PhD
Chair

Dr. H. Abdulla, PhD
Committee Member

Dr. J. Conkle, PhD
Committee Member

December 2019

ABSTRACT

This study represents the first comprehensive analysis of wet deposition ethanol in the Eastern US and South Texas to better comprehend how ethanol emissions are affecting atmospheric ethanol concentrations. Ethanol concentrations measured in 204 wet deposition samples collected at five Atmospheric Integrated Research Monitoring Network (AIRMoN) sites in the Eastern US between February 2018 to January 2019 ranged from below the detection limit of 19 nM to 4160 nM and concentrations measured in 48 rain events in South Texas during the same time period ranged from below the detection limit to 13195 nM. The volume weighted average ethanol concentration of AIRMoN samples ranged from 208 nM to 1017 nM while the volume weighted average ethanol concentration in South Texas was 1177 nM. Adding the five AIRMoN data to the previous empirical-based global wet deposition flux estimated by using data from 12 sites globally, the global wet deposition ethanol flux was estimated to be 2.7 ± 1.3 Tg/yr. No significant correlation was observed between ethanol and any analytes (NH_4^+, Cl^-, SO_4^{2-}, NO_3^-, Ca^{2+}, Na^+, Mg^{2+}, K^+, PO_4^{3-} and H^+) in almost all sites in the study, likely due to the difference in atmospheric residence time and emission sources. When investigating AIRMoN data as a whole, a significant correlation was observed between ethanol and chloride and ethanol and sodium ion concentration, suggesting common inputs from forest or marine sources. Significant seasonal variations of ethanol were not observed for any sites, which suggest a continuous emission of ethanol to the atmosphere. Anthropogenic and biogenic (with and without C4 plants) contributions to atmospheric ethanol were estimated using ISOERROR and SIAR isotope mixing models. Excluding C4 plants in the models, our results suggest that the greater fraction of ethanol in South Texas (ISOERROR: 70.6 ± 12.8%; SIAR: 68.4 ± 12.7%) and NY67 (ISOERROR: 66.1 ± 11.9%; SIAR: 63.4 ± 12.9%) was

emitted from anthropogenic sources; the contribution of biogenic (ISOERROR: 49.6%; SIAR: 52.2 ± 12.7%) and anthropogenic (ISOERROR: 50.4%; SIAR: 47.8 ± 12.7%) sources was equivalent in WV99 while the biogenic (ISOERROR: 63.2 ± 8.3%; SIAR: 60.4 ± 16.5%) sources contribution was dominant in TN00. Including C4 plants in the models, our results suggest that the greater fraction of ethanol in South Texas (ISOERROR: 58.1 ± 14.8%; SIAR: 56.9 ± 16.0%) and NY67 (ISOERROR: 63.4 ± 12.6%; SIAR: 58.3 ± 19.5%) was emitted from anthropogenic sources; the contribution of biogenic sources was dominant in TN00 (ISOERROR 74.2 ± 10.1%; SIAR: 67.2 ± 18.3%) and WV99 (ISOERROR 70.7%; SIAR: 67.8 ± 14.8%). Therefore, as the distribution of C3 and C4 plants varies from site to site, this study suggests that it is important to consider the types of plants around each site before assigning the representative endmember value for biogenic sources. Results of this study are important as it provides atmospheric scientists, environmental chemists and policy makers with a baseline of atmospheric ethanol concentration in order to help determine the efficacy of future ethanol fuel use and to help quantify the wet deposition ethanol sink. As ethanol fuel consumption and thereby emissions are increasing globally, it is important to understand the magnitude of all ethanol sources and sinks and their impacts in the atmosphere.

ACKNOWLEDGEMENTS

I would like to thank my committee chair, Dr. J. David Felix, and my committee members, Dr. Hussain Abdulla, and Dr. Jeremy Conkle for their guidance and support throughout this project. I would also like to thank the AIRMoN operators and supervisors namely Thomas Butler, LaToya Myles, David Gay, Rick Artz, Ariel Stein, Julie Dzaak, David Stensrud, Chris Lehmann, Bob Ziegler and Simone Klemenz for collecting and shipping samples. Isotopic analysis was made possible with the help from University of North Carolina, Wilmington and I would like to thank all associated researchers at the university. I would finally like to thank Alexander Berner, Warren Dunegan, Scilyn Apacible and all my friends and colleagues who volunteered their time and provided valuable insights for this research.

LIST OF FIGURES

LIST OF TABLES

1. INTRODUCTION

Ethanol is an oxygenated volatile organic compound (OVOC) that occurs naturally in the environment and is biologically and chemically labile [*Kirstine and Galbally*, 2012a]. Ethanol is preferred in the energy industry because it is a renewable source of energy, and the internal combustion engines of vehicles that use petroleum require minimal modifications in order to use ethanol in a fuel mixture [*Kirstine and Galbally*, 2012a]. The overuse of fossil fuels may lead the world towards fuel scarcity because of the limited fossil fuel reservoirs, while the production and use of biofuels like ethanol offers a sense of global fuel security and sustainability. In the US, ethanol was used in a fuel mixture as E10 (10% ethanol by volume) for the first time in 1978 and its production has increased exponentially since then (Figure 1) [*Renewable Fuels Association*, 2018; *U.S. Energy Information Administration*, 2016]. The US Renewable Fuel Standard has a mission to produce 36 billion gallons of renewable fuel in 2022 to reduce the emission of greenhouse gases like carbon dioxide and the dependency on fossil fuels [*Renewable Fuels Association*, 2018]; thus, more than doubling the current biofuel production of about 16 billion gallons [*Renewable Fuels Association*, 2018]. Currently, gasoline containing some quantity of ethanol as an additive in the US fuel market is more than 98% [*US Department of Energy*, 2018]. As the production and emission of ethanol is increasing, sixty-four countries have already established their mandates for biofuel production [*Goldemberg et al.*, 2014]. An increase in the global ethanol production has led to ethanol emission increase due to partially combusted fuels and has triggered many studies to investigate ethanol fuel consumption [*Poulopoulos et al.*, 2001]. A recent study done in North Carolina shows that the gaseous and wet deposition ethanol has increased by approximately fourfold in eight years, implying that the existing sinks for

atmospheric ethanol are not sufficient and the rate of addition of ethanol in the atmosphere is greater than the rate of its removal [*Willey et al.*, 2019].

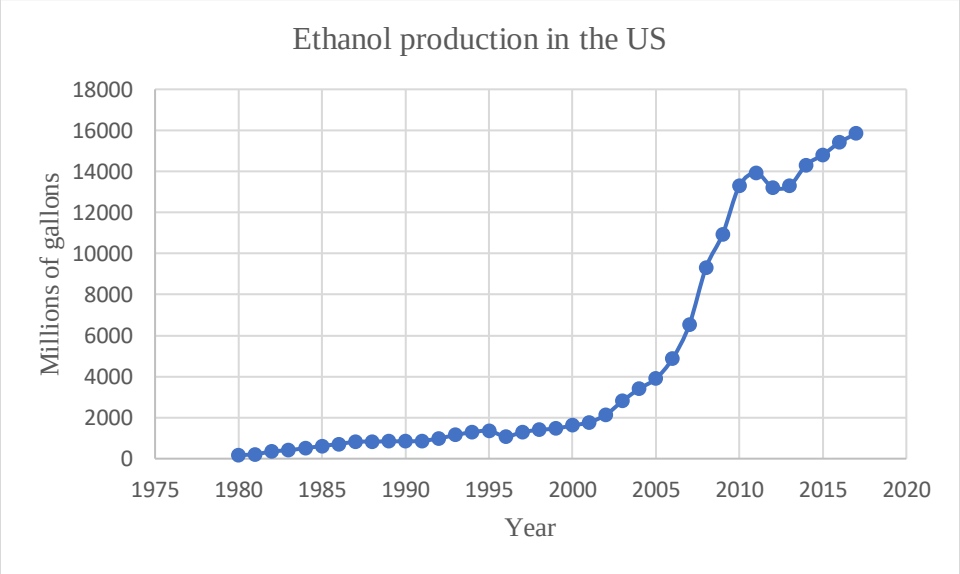

Figure 1. Ethanol production in the US from 1980 to 2017 [Renewable Fuels Association, 2018]

A majority of the ethanol studies have focused on acetaldehyde and formaldehyde as they are produced from ethanol fuel combustion and are carcinogenic in nature [*Giebel et al.*, 2011]. Also, aldehydes are sources of peroxyacetyl nitrate, and both of these compounds aid in the formation of tropospheric ozone and smog [*Naik et al.*, 2010; *Salvo and Geiger*, 2014]. The reaction of ethanol with hydroxyl and hydroperoxyl radicals also have implications in aerosol formation and greenhouse radiative forcing [*Guenther et al.*, 1995].

Biogenically, ethanol is produced by plants as it aids in cell repair, growth and development [*Kirstine and Galbally*, 2012a]. Almost all plants are able to produce ethanol in hypoxic or anoxic environments and environmental stresses like flooding [*Copolovici and Niinemets*, 2010], frost [*Fukui and Doskey*, 1998], drought [*Manter and Kelsey*, 2008] and chemical exposures [*MacDonald et al.*, 1989] trigger plants to produce ethanol. In oxygen-deficient conditions, plants shift the process of mitochondrial respiration to ethanolic fermentation [*Jardine et al.*,

2010], thereby producing ethanol as a product [*Kirstine and Galbally*, 2012a]. Further natural processes like herbivory, biomass burning and death and decay of organisms can also contribute to ethanol emission in the atmosphere [*Kirstine and Galbally*, 2012a].

A few studies have detailed the fate and transport of ethanol in soil and groundwater. Agreements among these studies suggest that the ethanol in soil is less likely to get volatilized when it is trapped in an aqueous phase. The ethanol, thus trapped, is also unlikely to reach toxic level as most of it gets degraded by microbes within a few days. Though the concentration of ethanol in water bodies would be low, it has a tendency to decrease the oxygen levels in the surface or groundwater, thus impacting in the respiration of aquatic bodies [*Kirstine and Galbally*, 2012a].

A large discrepancy is observed in the estimates of global ethanol source contribution in different literatures. For instance, the estimates for total ethanol emission sources are 8 – 17 Tg/ yr [*Singh et al.*, 2004], 15 Tg/yr [*Naik et al.*, 2010], 25 Tg/yr [*Millet et al.*, 2012] and 25 – 56 Tg/ yr [*Kirstine and Galbally*, 2012a]. The average reported value for global ethanol emissions from vegetation ranges from 6 – 26 Tg/yr, and that from anthropogenic sources ranges from 2 – 6 Tg/yr [*Kirstine and Galbally*, 2012a; *Millet et al.*, 2010; *Naik et al.*, 2010; *Singh et al.*, 2004]. The estimates of global ethanol sinks also exhibit large discrepancies as their values range from 15 – 70 Tg/yr [*Felix et al.*, 2017; *Kirstine and Galbally*, 2012b; *Naik et al.*, 2010].

Ethanol has a residence time of 2.8 days in the atmosphere [*Naik et al.*, 2010] and it is removed from the atmosphere by three major processes: reaction with hydroxyl radicals, dry and wet deposition [*Felix et al.*, 2017; *Giebel et al.*, 2011; *Kirstine and Galbally*, 2012a; *Naik et al.*, 2010]. The primary removal process is oxidation, however wet and dry deposition also play an important role in removal. The tendency of ethanol to make a strong hydrogen bond with water

aids in removal via precipitation [*Naik et al.,* 2010]. A recent study using empirical data calculated the global ethanol wet deposition flux to be 2.4 ± 1.6 Tg/yr [*Felix et al.*, 2017] which complies with modelled range for global wet deposition of ethanol (1.4 – 5.0 Tg/yr) [*Felix et al.*, 2017; *Kirstine and Galbally*, 2012b; *Naik et al.*, 2010]. However, this empirical study only focused on 12 sites globally and lacked high temporal resolution. Therefore, there is still a major gap in the quantification of the ethanol wet deposition flux.

Carbon isotopic analysis can be used to determine the sources of various carbon containing compounds including ethanol [*Sharp,* 2017]. Isotopes are different forms of a same element that vary due to the difference in the number of neutrons [*Sharp,* 2017]. The $\delta^{13}C$ value of ethanol from biogenic sources differs from the $\delta^{13}C$ value of ethanol from anthropogenic sources; and using this property, the percentage contribution of ethanol from these two sources can be calculated [*Felix et al.,* 2017; *Giebel et al.,* 2011; *Keppler et al.,* 2004]. Isotopic fractionation, defined as a phenomenon of partitioning isotopes between two substances or two forms of a same substance with varying isotope ratio, plays a vital role in stable isotopes research [*Hoefs and Hoefs,* 1997]. If the fractionation is minimum, the $\delta^{13}C$ value of ethanol does not vary significantly from that of the source and vice-versa. For example: a recent study shows that the $\delta^{13}C$ value of ethanol from US vehicle exhaust was -9.8 ± 2.5‰, close to that of the corn ethanol (-10.7 ± 0.31‰) added to US fuel due to minimal fractionation [*Felix et al.,* 2018].

To determine the spatial and temporal variation of ethanol concentration in Eastern US and South Texas, this study sampled wet deposition samples from six sites on an event basis for a year in a collaboration with the National Atmospheric Deposition Program's (NADP) Atmospheric Integrated Research Monitoring Network (AIRMoN). The data provides atmospheric scientists, environmental chemists and policy makers with a baseline of atmospheric

ethanol concentration in order to help determine the efficacy of future ethanol fuel use. This study also determined the correlation between ethanol concentration, pH and various ions in wet deposition to find the common sources of ethanol and other analytes. Further confirmation and categorization of ethanol sources was performed in the study by using airmass back trajectories. The seasonal variation of ethanol was also studied and the percent contribution of anthropogenic and biogenic sources of ethanol was estimated by measuring the isotopic composition of ethanol in a small subset of wet deposition samples. As the anthropogenic and biogenic emission sources of ethanol have different isotopic signatures, this study used isotopic analysis to determine the sources of ethanol.

2. METHODS

2.1 Study Sites Overview

Wet deposition at six different sites in the US were sampled; five sites are part of National Atmospheric Deposition Program's (NADP's) Atmospheric Integrated Research Monitoring Network (AIRMoN) and the sixth is in South TX (Texas A&M University-Corpus Christi). Samples were collected for a period of 1 year starting from February 2018 to January 2019 except in Illinois and Pennsylvania where the samples were collected from February 2018 to May 2018. NADP sites are located in rural areas, thus minimizing impacts from local point sources and are meant to provide representative data of regional wet deposition chemistry [*Bigelow et al.*, 2001]. The five AIRMoN sites were used for the US East Coast study and the sixth site is used for Texas study. These AIRMoN sites were chosen in the study because they are the only NADP sites that collect wet deposition samples on an event basis. The collection of samples on an event basis is crucial in this study because ethanol, being a volatile organic compound, will volatilize from the

sample relatively quickly. It is also biologically labile and can be used by organisms in the sample if not collected immediately. The identity of all study sites is given in Table 1 and shown in Figure 2.

Table 1. Identity of the study sites (Population is based on [US Department of Commerce, 2010])

States	**AIRMoN Site ID**	**Cities/ Towns**	**Latitude**	**Longitude**	**Population**
Texas	N/A	Corpus Christi	27.7147	-97.3286	305,215
Illinois	IL11	Bondville	40.0528	-88.3719	443
Pennsylvania	PA15	State College	40.7883	-77.9458	42,034
New York	NY67	Ithaca	42.4014	-76.6589	30,014
Tennessee	TN00	Oak Ridge	35.9614	-84.2872	29,330
West Virginia	WV99	Davis	39.1191	-79.4522	660

2.2 Study Site Description

Site 1, Texas A&M University-Corpus Christi lies in Corpus Christi, TX. The average annual high and low temperature of Corpus Christi is 27.5 °C and 17.11 °C respectively while the average annual rainfall is 805.18 mm [*US Climate Data*, 2018a]. Site 2 or IL11 of AIRMoN site is located in Bondville, IL. Bondville is a small town with an area of 0.66 squared-km [*United States Census Bureau*, 2016]. Its annual average temperature is 10.67 °C and annual precipitation is 995.93 mm [*World Media Group*, 2018a]. Site 3, PA15 is located in State

College, PA. A grain processing plant that produces 110 million gallons of ethanol per year [*Pennsylvania Grain Processing*, 2019] is situated at ~ 48 km from the wet deposition collection site. The average annual maximum and minimum temperature of State College, PA is 15.06 °C and 5.17 °C respectively while the average annual rainfall of the region is 1005.84 mm [*US Climate Data*, 2018c]. State College also bears 1143 mm of snowfall annually [*US Climate Data*, 2018c]. Site 4, NY67 is located in Ithaca, NY. The average annual maximum and minimum temperature is respectively 13.61 °C and 2.67 °C [*US Climate Data*, 2018b]. The annual precipitation as a rainfall in Ithaca is 947.42 mm and as snowfall is 1651 mm [*US Climate Data*, 2018b]. Site 5, TN00 is located in Walker Branch Watershed, TN in the US Department of Energy's Oak Ridge Reservation. The average high and low temperatures of Oak Ridge is 20.83 °C and 8.44 °C respectively [*US Climate Data*, 2018d]. The annual precipitation as a rainfall and snowfall in that area is respectively 1409.95 mm and 177.8 mm [*US Climate Data*, 2018d]. Site 6, WV99 is located in Canaan Valley Institute, Davis, WV. The average maximum and minimum

temperature of Davis is respectively 12.94 °C and 2.67 °C [*US Climate Data*, 2018e]. The average annual rainfall in Davis is 1357.12 mm [*World Media Group*, 2018b].

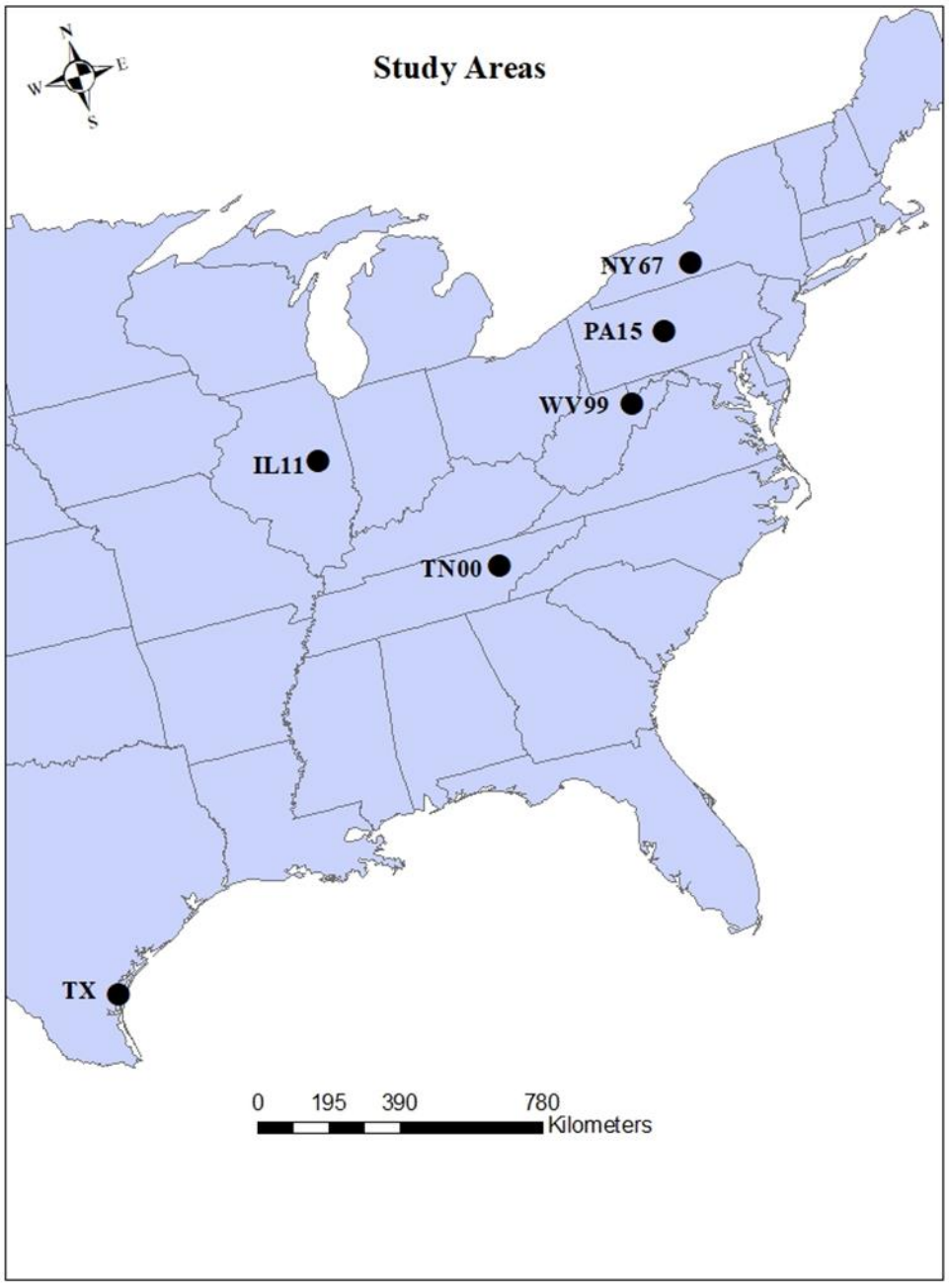

Figure 2. Location of wet deposition collection sites in the study. The five sites in the Eastern US represent AIRMoN sites while the sixth site represents South Texas.

2.3 Wet Deposition Sample Collection and Preservation

Wet deposition samples were collected on an event basis since December 2016 in South Texas and from February 2018 to January 2019 at the five AIRMoN sites. The collection of samples was done at five AIRMoN sites by using Aerochem-Metrics (ACM) Model 301 Automatic Sensing Wet/Dry Precipitation Collectors and by using N-CON 00-120 deposition sampler at Texas A&M University-Corpus Christi. At AIRMoN sites, the samples were collected using a bag sampling method where a bag liner is attached to a bucket for wet deposition collection [*NADP*, 2018]. The sample was then decanted to a 40 mL vial containing 70 µL of mercury (II) chloride ($HgCl_2$). A travel blank was also sent while shipping the vials to the AIRMoN sites. Prior to using any beakers and glassware for the collection and filtration at Texas A&M University-Corpus Christi, they were kept in acid-bath (10%) for at least 30 minutes and rinsed with Millipore MQ deionized water (> 18 MΩ/cm) and combusted in a muffle furnace at 450°C for a minimum of 4.5 hours to eliminate organics. Immediately after the wet deposition event, samples were brought back to the laboratory and filtered. The filtration was done using 0.2 µm Gelman Supor® polysulfonone filters. All the samples were preserved in 40 mL glass vials containing 70 µL of $HgCl_2$ and kept in a refrigerator at 4°C. The $HgCl_2$ is known to preserve ethanol in wet deposition samples for at least 160 days [*Felix et al.*, 2017].

2.4 Ethanol Concentration Analysis

Ethanol concentration in wet deposition was measured using solid-phase microextraction (SPME) gas chromatography – flame ionization detection [*Kieber et al.*, 2013]. In summary, 11.6 mL of wet deposition sample aliquot was added to a 20 mL vial containing 3.5 g of NaCl. It was then buffered to a final pH of 4.4 by the addition 400 µL of a succinate buffer. The buffer was prepared by adding 16.7 ml of 0.2 M sodium hydroxide in 25 mL of 0.2 M succinic acid and

diluting it to a total of 100 mL. The sample was heated and stirred at 50 °C for 10 minutes prior to a 20-minute extraction by a 75 μm Carboxen/PDMS (Polydimethylsiloxane) SPME fiber in the headspace (HS) region. Magnetic stirring was required during preheating as well as during extraction phase at a rate of 750 rpm. After extraction, the fiber was thermally desorbed in the injection port of the GC-FID for concentration analysis.

2.5 GC-FID Conditions

A Thermo Scientific Trace 1310 GC equipped with a Restek®-5 (30 m x 0.32 mm x 1 μm) or Equity-5 (20 m x 0.32 mm x 0.32 μm) fused-silica capillary column and a Merlin microseal adapter was mounted on the GC injection port. The oven temperature began at 35°C and ramped to 60°C at 5°C/min and held for 1 minute before heating to a final temperature of 200°C at 60°C/min and held for 2 minutes [*Guy*, 2013; *Kieber et al.*, 2013].

The injection port of the GC-FID equipped with a Merlin SPME Microseal septum and held at a constant temperature of 230°C with a constant helium pressure of 3.2 psi was operated in the splitless injection mode. Following the extraction period, the fiber was thermally desorbed for 1 minute in the injection port. Analytes were detected using a flame ionization detector set at 250°C [*Guy*, 2013; *Kieber et al.*, 2013].

2.6 NH_4^+ Concentration Analysis

The analysis for NH_4^+ was done using the orthophthaldialdehyde (OPA) method by [*Holmes et al.*, 1999]. This method involves preparation of a working solution by using three reagents. 1 g of OPA was dissolved in 25 mL of ethanol to prepare the OPA solution, 10 g of sodium tetraborate was dissolved in 250 mL of Milli-Q to make a borate solution and 0.8 g of sodium sulfite was dissolved in 100 mL of Milli-Q to prepare a sodium sulfite solution. Then, 0.5 mL of the sulfide

solution and 5 mL of the OPA solution was added to 94.5 mL of the borate solution to make 100 mL of working solution. This was followed by the preparation of eight different NH_4^+ standards. 1 mL of the working solution was added to 0.25 mL of each standard/sample added to an individual cuvette. The solution was uniformly mixed and kept in the dark for 3 hours to ensure the reaction. The concentration of NH_4^+ was then determined using a Trilogy® Laboratory Fluorometer.

2.7 Anion Analyses

Anion concentrations (e.g. chloride, sulfate, nitrite and nitrate) were measured in the study using ion chromatography. Briefly, five different concentration (0.1 ppm, 1 ppm, 5 ppm, 10 ppm and 50 ppm) of anion standards were prepared using Dionex™ ion standard solution. 1 mL of a standard/sample was added to a tube required for a Dionex™ Ion Chromatograph 4000i/ AS-AP autosampler and the samples were run for 23 minutes per run at a flow rate of 1 mL/min. The ion chromatograph has an AS4A separation column and an elutant consisting 1.8 mM Na_2CO_3 + 1.7 mM $NaHCO_3$.

2.8 Ancillary data

The measurements for analytes like NH4+, Cl-, NO3-, Ca2+, Na+, Mg2+, PO43- and H+ of AIRMoN samples were performed by the Central Analytical Laboratory at the University of Wisconsin. Information for stringent QA/QC and methodology can be found: http://nadp.slh.wisc.edu/QA/.

2.9 Carbon Isotope Analysis of Ethanol

A small subset (n = 9) of samples with high ethanol concentration (>750 nM) were sent to University of North Carolina – Wilmington (UNCW) for isotopic analysis. Out of these, 3 were from Texas, 3 from Tennessee, 2 from New York and 1 from West Virginia. The small subset was a result of sample damage (n = 41) during shipping to the isotope facility.

2.9.1 Pre-injection GC-C-IRMS Conditions

A Thermo Trace 1310 GC was equipped with a Restek®-5 (30 m x 0.32 mm x 1 μm) fused-silica capillary column and a Merlin microseal adapter was mounted on the GC injection port. A Taylor-Wharton 25 L liquid nitrogen Dewar was equipped with a liquid withdrawal device connected to the back of the GC oven by a copper pipe to allow for sub-ambient temperatures. Sub-ambient temperatures focus the ethanol upon injection leading to improved chromatography and separation.

After ethanol was extracted via the SPME method described previously, the SPME fiber was then introduced to the GC-C-IRMS via the Merlin microseal septum encased in the microseal adapter mounted in the GC injection port. The oven temperature was held for 3 minutes at 10°C before being ramped to 60°C at 10°C/min and heated to the final temperature of 200°C at 60°C/min and held for 2 minutes. Eluents were carried to a Thermo Isolink II device via the helium carrier gas where they were combusted at 1000°C in the presence of nickel oxide and platinum wires in an alumina ceramic reactor tube. Resulting CO_2 was analyzed in a continuous-flow mode via an interfaced Thermo Delta V plus stable isotope mass spectrometer at the University of North Carolina Wilmington – Isotope Ratio Mass Spectrometry (UNCW-IRMS) Facility.

The vacuum system of the IRMS was maintained at a constant operating source pressure of 4.9 x 10^{-8} mbar. Standards and samples were calibrated daily against a working CO_2 reference gas versus the international Vienna PeeDee Belemnite (V-PDB) standard (equation 1).

$$\delta^{13}C_{sample} = [(^{13}C/^{12}C)_{Sample} / (^{13}C/^{12}C)_{V\text{-}PDB} - 1] \times 1{,}000 \quad (1)$$

Two ethanol isotope standards were used to apply a two-point normalization to the V-PDB scale [*Coplen et al.,* 2006]. The standards were purchased from the stable isotope reference program at Indiana University's Biogeochemical Laboratories ($\delta^{13}C$ values of -10.98 ± 0.02‰ and -27.53 ± 0.02‰).

2.9.2 Source Apportionment

A two-end member mixing model as shown in equation 2 was used to determine ethanol emission source contribution to wet deposition. EPA ISOERROR was used to calculate the percent contribution of different sources to wet deposition ethanol concentration using their isotopic signatures [*Phillips and Gregg,* 2001]. The ISOERROR user is required to provide sample $\delta^{13}C_{EtOH}$ values with standard deviations and source endmember $\delta^{13}C_{EtOH}$ values with standard deviations for determining the uncertainty. The biogenic endmember $\delta^{13}C_{EtOH}$ value was obtained from available literature and the $\delta^{13}C_{EtOH}$ values for C3 plants (-30.9 ± 4.2‰ (n =15)) was considered as a biogenic endmember [*Giebel et al.,* 2011; *Keppler et al.,* 2004]. The biomass of C3 plants contributes ~95% of the world's total C3 + C4 biomass; therefore C3 plants emission was chosen as an indicator for biogenic endmember signatures [*Still et al.,* 2003]. The US vehicle endmember value of -9.8 ± 2.5‰ (n = 4) was used as an anthropogenic endmember value [*Felix et al.,* 2018]. Since ethanol in vehicular fuel is from distilleries, we are assuming that the vehicular and distilleries emission signatures would be same due to minimal

fractionation during ethanol fuel combustion [*Felix et al.*, 2018]. Other endmembers (For instance: marine sources, biomass burning, C4 plants) were assumed to contribute negligibly, and their $\delta^{13}C_{EtOH}$ values have not been well illustrated yet [*Giebel et al.*, 2011]. The mixing model required for determining the contribution from anthropogenic and biogenic sources is shown in equation 2.

$$\delta\ ^{13}C_{Sample} = f\ (\delta\ ^{13}C_{Biogenic}) + (1-f)\ (\delta\ ^{13}C_{Anthropogenic}) \qquad (2)$$

where f = fraction contribution from biogenic sources.

Previous studies in atmospheric ethanol only considered the carbon isotopic signature of C3 plants as a biogenic endmember value as described above. This study also considers a second mixing model which includes the carbon isotopic endmember value of C4 plants in the biogenic endmember value. The two-end members mixing model using a C3/C4 combination was used to calculate the biogenic end member value for each site (equation 3). The $\delta^{13}C_{EtOH}$ value for C4 plants used in this study is -15.2 ± 0.5‰ (n = 1) [*Keppler et al.*, 2004]. The C3/C4 plant ratio for all states were derived from a study on the distribution of C3 and C4 vegetation [*Still et al.*, 2003] (Table 2). After calculation of $\delta^{13}C$ value for ethanol emitting from biogenic sources using equation 3, it was used in equation 2 to determine the contribution from biogenic and anthropogenic sources in each site.

$$\delta\ ^{13}C_{Biogenic} = f\ (\delta\ ^{13}C_{C3}) + (1-f)\ (\delta\ ^{13}C_{C4}) \qquad (3)$$

where f = fraction contribution from C3 vegetation.

Table 2. Distribution of C3 and C4 plants in all study sites [*Still et al.*, 2003]

Sites	Fraction of C3 plants	Fraction of C4 plants
Texas	0.6	0.4
TN00	0.8	0.2

WV99	0.6	0.4
NY67	0.9	0.1
IL11	0.6	0.4
PA15	0.8	0.2

Moreover, for comparison study between SIAR (Stable Isotope Analysis in R) model and ISOERROR, the percentage contribution was also determined using SIAR package in R software. The SIAR package uses isotopic signatures and determines the sources contribution based on Bayesian model while ISOERROR uses frequentist statistics to predict its results. In frequentist model, statistical parameters are estimated using sampling distribution and are considered as fixed but unknown quantities. However, in Bayesian model, statistical parameters are estimated using probability distribution and are treated as random variables [*Guyon et al.*, 2010].

2.9.3 HYSPLIT Back Trajectories Model

Air – mass back trajectories for each wet deposition event were developed by using the Hybrid Single Particle Lagrangian Integrated Trajectory (HYSPLIT) model from National Oceanic and Atmospheric Administration (NOAA) [*National Oceanic and Atmospheric Administration*, 2018]. The back trajectories were produced starting at the end of the precipitation event for a 72 – hour hind – cast at an altitude of 500 m. As the estimated lifetime of ethanol is 2.8 days [*Naik et al.*, 2010], 72 hours was chosen as the time duration for back trajectories. 500 m altitude indicate the well-mixed boundary layer for air mass that is likely to contribute more heavily to in-cloud processes contributing to wet deposition [*Avery Jr et al.*, 2006].

For the five AIRMoN sites, the direction of airmass was divided as Northeast (NE), Southeast (SE), Southwest (SW), Northwest (NW) and mixed based on the back-trajectories. The directions were categorized as NE (0-90°), NW (90-180°), SW (180-270°), SE (270-360°) and "mixed" direction means the wind direction includes more than one specific direction (NE, NW, SW and SE).

The airmass was visually categorized as terrestrial, marine or mixed based on the origin and direction for the South Texas site as it is the only site in this study that can potentially have airmass with significant marine origin. If an airmass includes a large fraction of both land and water mass, it is categorized as "mixed" airmass origin.

2.10 Global Wet Deposition Flux

Adding AIRMoN data to the previously estimated global wet deposition flux dataset [*Felix et al.*, 2017], the new global wet deposition ethanol flux was estimated. All the sites were grouped into either "Terrestrial with no local source", "Terrestrial with local source" or "Marine source" categories. The VWA concentrations at each site in a group was simple averaged to calculate the VWA concentration for the group. Standard deviation of the group VWA concentration was used to calculate the maximum and minimum values for the global wet deposition flux. Secondary data for global areas and deposition amount were taken from [*Peixoto and Oort*, 1992] and the areas with high local sources/urban areas were estimated from [*American Association for the Advancement of Science*, 2019].

3. RESULTS

The ethanol concentration was measured in 252 wet deposition samples out of which 16 concentrations were outliers. Outliers are calculated based on interquartile range. If an ethanol

concentration is greater than 1.5 times the interquartile range plus the third quartile of a dataset, the value is considered as an outlier.

3.1 AIRMoN Sites

3.1.1 Wet deposition ethanol concentration (AIRMoN)

The volume-weighted average (VWA) concentration of wet deposition ethanol was maximum for PA15 (1017 nM, n =16) followed by IL11 (687 nM, n = 10), TN00 (410 nM, n = 44), WV99 (352 nM, n = 56) and NY67 (208 nM, n = 78) (Figure 3).

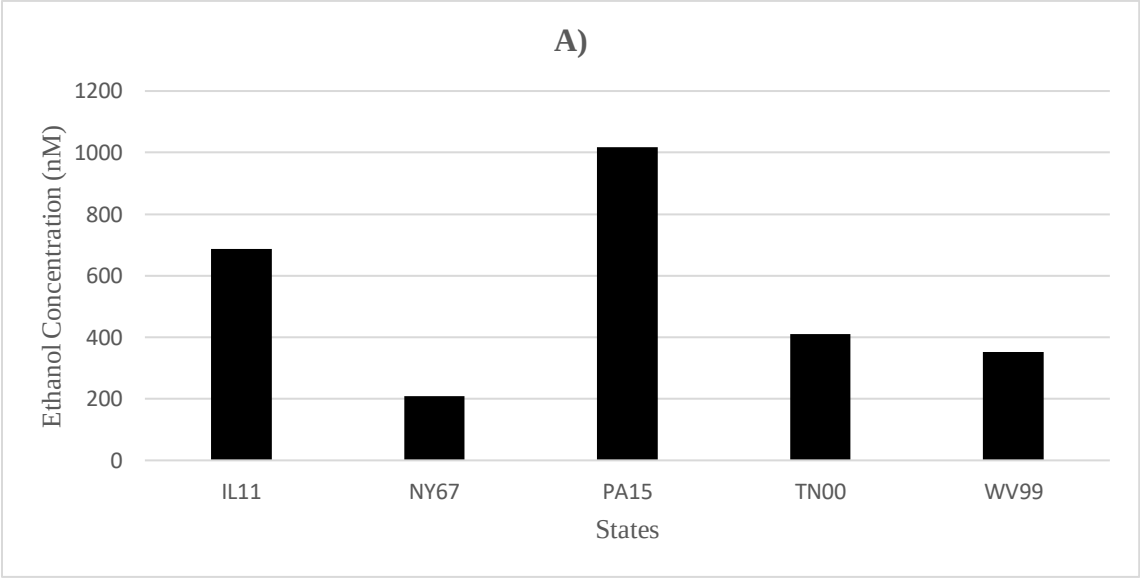

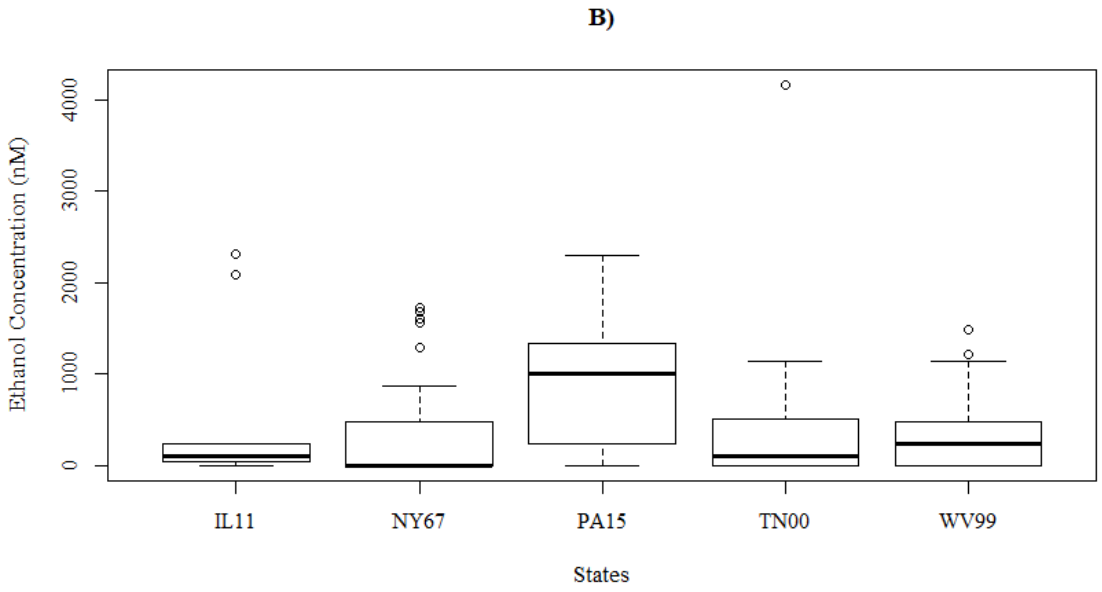

Figure 3. A) VWA wet deposition ethanol concentration in AIRMoN sites in this study. B) Box and whisker plot of wet deposition ethanol concentration in all AIRMoN sites in the study. Black horizontal dashed line inside the box represents the median, the box represents the interquartile range, the end bars represent the range and the circles represent the outliers in the data.

3.1.2 Seasonal variation of ethanol concentration (AIRMoN)

Seasonal wet deposition ethanol data were compiled based on seasonal quarters where quarters are defined as winter (January 1 – March 31), spring (April 1 – June 30), summer (July 1 – September 30) and fall (October 1 – December 31) (Figure 4). An ANOVA test ($\alpha = 0.05$) was performed to see whether there is any correlation between ethanol concentration according to seasons at the study sites. Though some differences in concentration of wet deposition ethanol according to seasons were observed, not a single site showed a statistically significant variation according to seasons (ANOVA, p – value > 0.05).

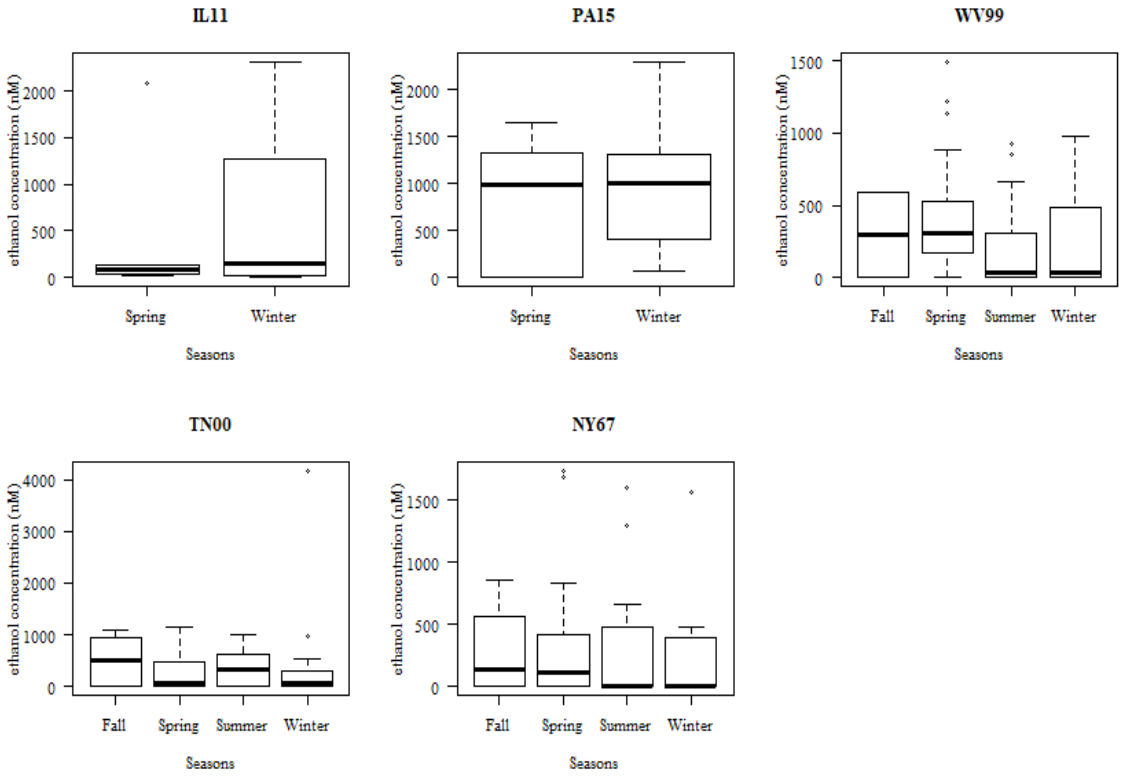

Figure 4. Box and whisker plot of seasonal variation of wet deposition ethanol concentration at AIRMoN sites. Black horizontal dashed line inside the box represents the median, the box represents the interquartile range, the end bars represent the range and the circles represent the outliers in the data.

The seasonal variation of VWA wet deposition ethanol concentration was also calculated for all combined AIRMoN sites in the study. No statistically significant seasonal variation was observed in AIRMoN site samples (ANOVA, $\alpha = 0.05$). However, it was observed that the VWA wet deposition ethanol concentration was minimum in summer and maximum in winter (Figure 5). The seasonal variation of VWA wet deposition ethanol concentration for individual sites was also determined in the study (Appendix 1).

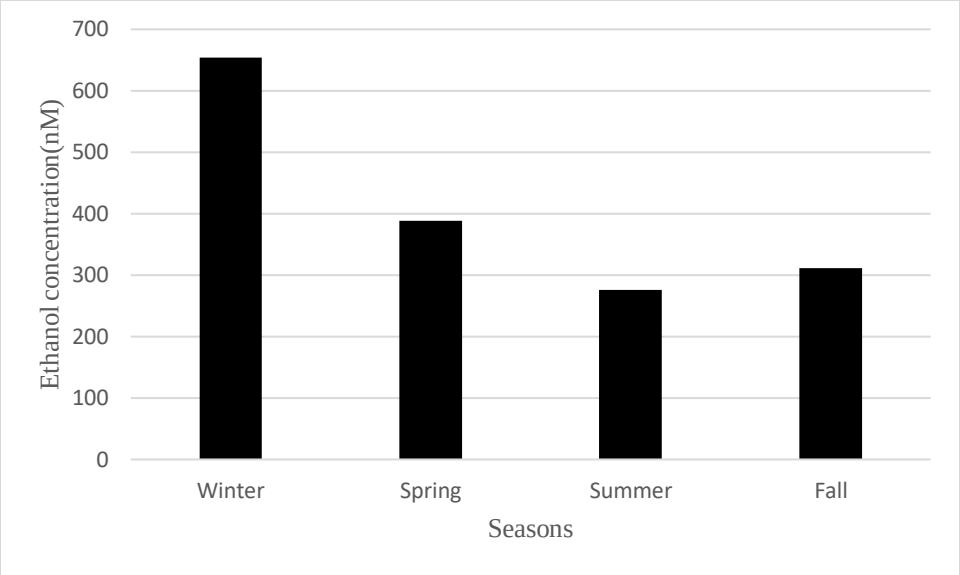

Figure 5. Seasonal variation in VWA ethanol concentration in AIRMoN sites.

3.1.3 Ethanol concentration variation according to airmass origin (AIRMoN)

Rain events at AIRMoN sites were classified as NE, NW, SW, SE or mixed based on back trajectories (Figure 6). To see if there's a correlation between wet deposition ethanol and airmass origin, ANOVA ($\alpha = 0.05$) test was performed. No sites showed a statistically significant correlation between wet deposition ethanol concentration and airmass origin. The frequency of an airmass originating from a particular direction in all rain events at AIRMoN sites is tabulated in Appendix 2.

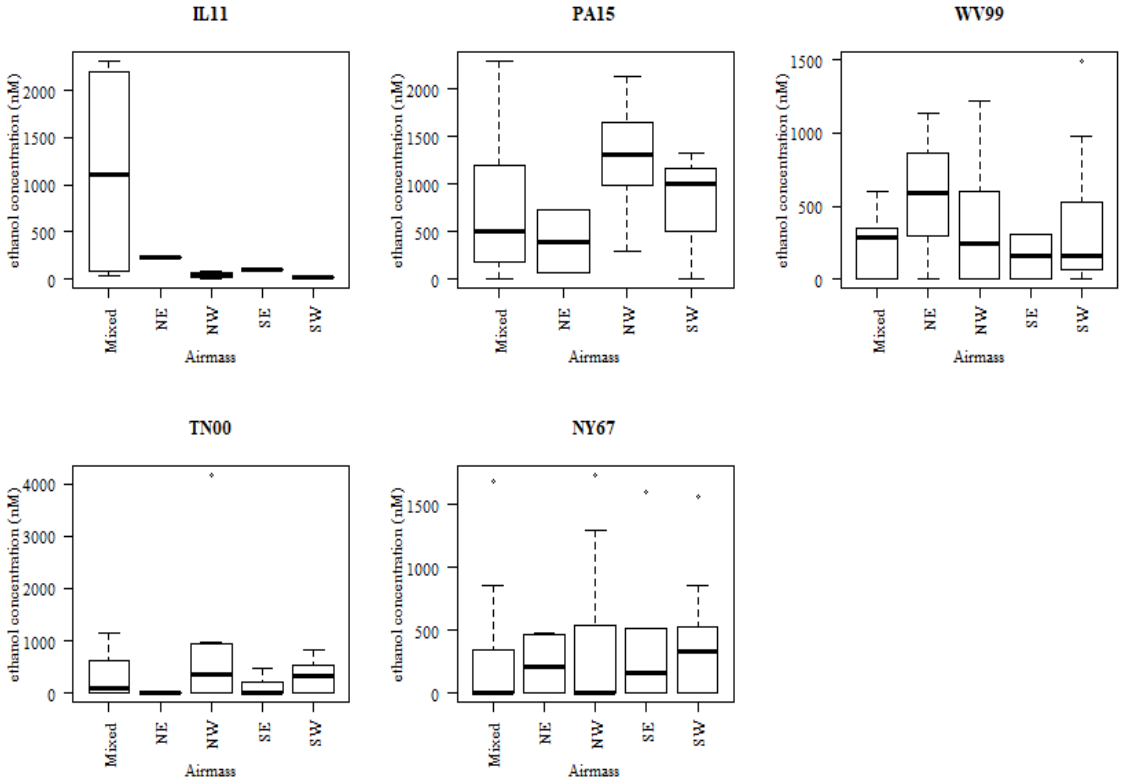

Figure 6. Box and whisker plots of variation of wet deposition ethanol concentration according to airmass origin. Black horizontal dashed line inside the box represents the median, the box represents the interquartile range, the end bars represent the range and the circles represent the outliers in the data

3.1.4 Ethanol concentration variation due to precipitation amount (AIRMoN)

There was no significant correlation between precipitation amount and the wet deposition ethanol concentration in all AIRMoN sites, suggesting that the rainout effect was not observed in this study (Figure 7). The individual sites were also studied separately but no correlation was observed between wet deposition ethanol concentration and precipitation amount (Appendix 3).

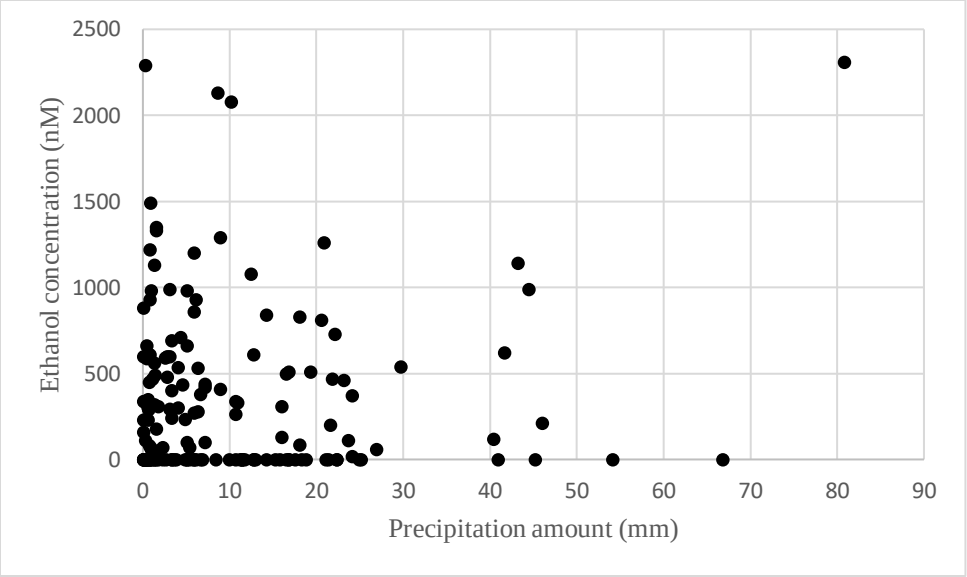

Figure 7. Variation of wet deposition ethanol according to precipitation amount in all AIRMoN sites. The absence of rainout effect suggests a continuous resupply of ethanol to the atmosphere.

3.1.5 Intercorrelation (AIRMoN)

All ancillary rainwater components were analyzed for intercorrelation using Pearson correlation analyses. No significant correlation was observed between ethanol and any other components in the wet deposition except chloride and sodium (Table 2). The correlations between ethanol and other wet deposition components were also analyzed for all AIRMoN sites individually (Appendices 4 – 8). A significant correlation between ethanol and phosphate was observed at TN00 and a significant correlation between ethanol and hydrogen ion was observed at WV99.

Table 3. Intercorrelation among ethanol, chloride, nitrate, sulfate, ammonium, hydrogen, calcium, magnesium, potassium, sodium and phosphate ions in wet deposition samples of all AIRMoN sites. Bold-faced values indicate significance at $p < 0.05$, $n = 113$

	Cl^-	NO_3^-	SO_4^{--}	NH_4^+	H^+	Ca^{++}	Mg^{++}	K^+	Na^+	PO_4^{---}
C_2H_5OH	**0.0018**	0.9916	0.1392	0.2461	0.0905	0.9163	0.9163	0.8335	**0.0256**	0.8747
Cl^-		**0.0002**	**<0.0001**	**0.0076**	0.9916	**0.0142**	**<0.0001**	**0.0026**	**<0.0001**	0.9163
NO_3^-			**<0.0001**	**<0.0001**	0.9832	**<0.0001**	**<0.0001**	**0.0027**	**0.0006**	**0.0027**

SO_4^{--}				**<0.0001**	0.2461	**<0.0001**	**<0.0001**	**<0.0001**	**<0.0001**	0.8747
NH_4^+					0.1392	**<0.0001**	**<0.0001**	**0.0001**	**0.0256**	**0.0256**
H^+						0.9163	0.9163	0.9163	0.8335	0.8335
Ca^{++}							**<0.0001**	**<0.0001**	**0.0001**	0.9163
Mg^{++}								**<0.0001**	**<0.0001**	0.8335
K^+									**<0.0001**	0.9163
Na^+										0.9163

3.2 South Texas Site

3.2.1 Wet deposition ethanol concentration (TX)

The VWA wet deposition ethanol concentration for the South Texas site was 1177 nM (n = 48) and the range of wet deposition ethanol concentration was below limit of detection (19 nM) to 13195 nM (figure 8).

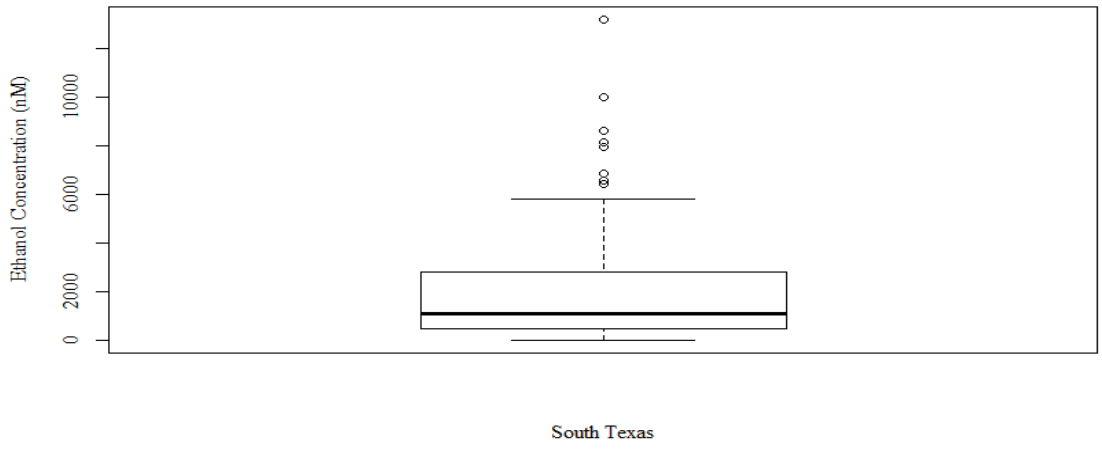

Figure 8. Box and whisker plot showing the wet deposition ethanol concentration in South Texas. Black horizontal dashed line inside the box represents the median, the box represents the

interquartile range, the end bars represent the range and the circles represent the outliers in the data.

3.2.2 Seasonal variation of wet deposition ethanol (TX):

The simple average concentration of wet deposition ethanol in fall at South Texas was significantly higher than that in summer (ANOVA, $\alpha = 0.05$, p – value = 0.04171, n = 48). However, no other seasons showed a significant variation in wet deposition ethanol concentration (Figure 9). The seasonal variation for VWA wet deposition ethanol concentration was also calculated for the South Texas site and the results show that the two seasons with maximum VWA ethanol concentration were fall and winter (Figure 10).

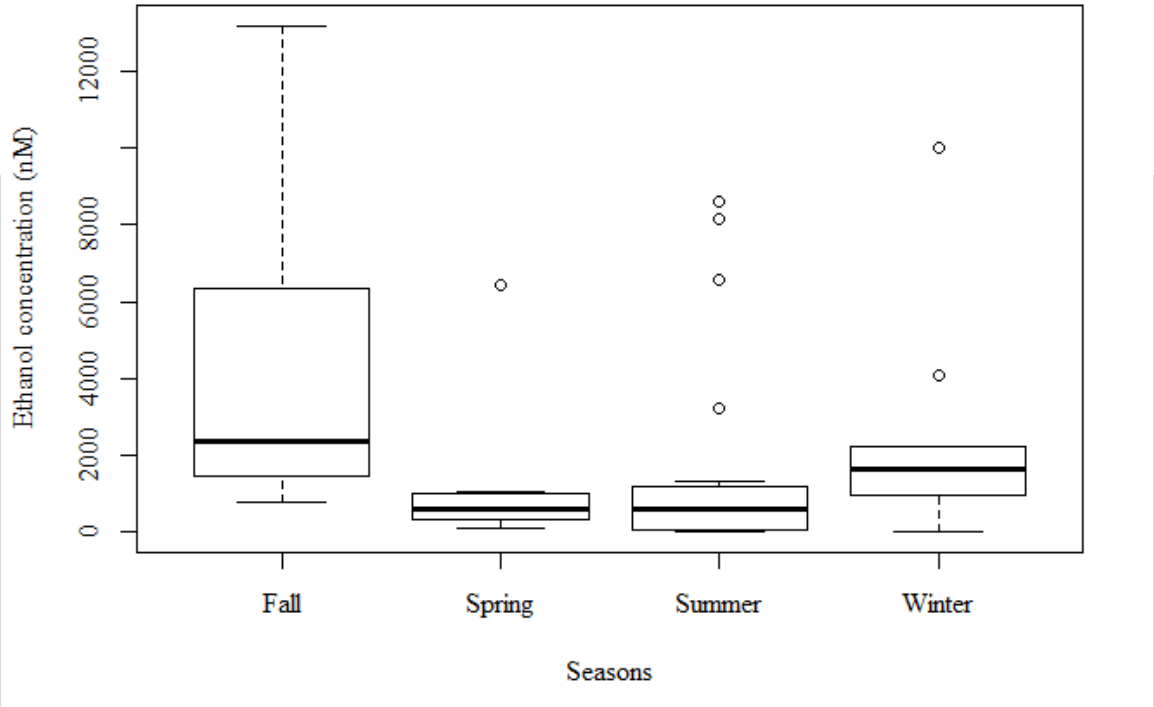

Figure 9. Box and whisker plot showing seasonal variation of wet deposition ethanol concentration in South Texas. Black horizontal dashed line inside the box represent the median, the box represents the interquartile range, the end bars represent the range and the circles represent the outliers in the data. The higher concentrations of wet deposition ethanol

concentration were observed in fall and winter while the lower concentrations were observed in spring and summer.

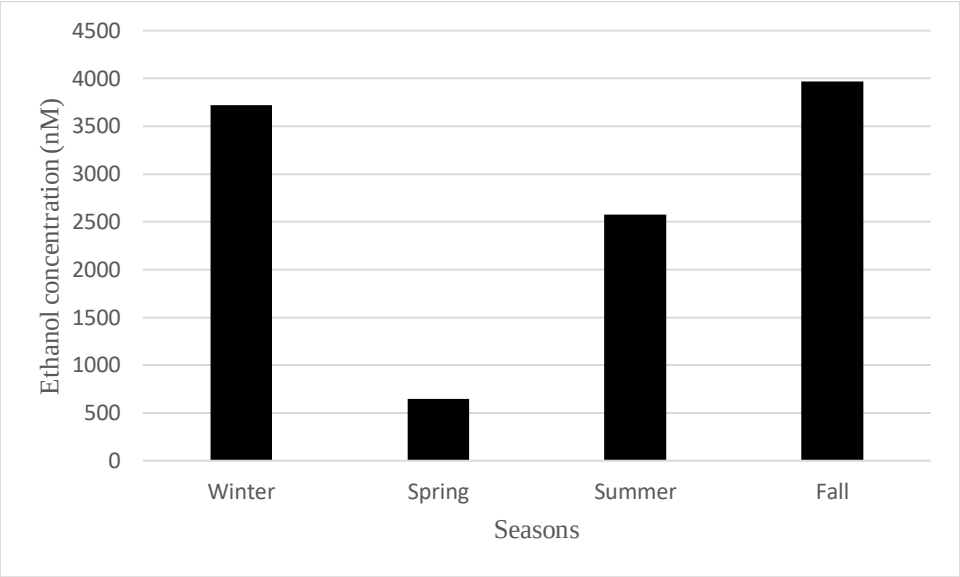

Figure 10. Seasonal variation in VWA ethanol concentration in South Texas. It was observed that the VWA wet deposition ethanol concentration was minimum in spring and maximum in fall.

3.2.3 Airmass origin (TX)

The wet deposition ethanol events were classified as NE, NW, SE, SW and mixed according to airmass origin. Furthermore, the rain events were also classified as terrestrial, marine or mixed to determine the continental influences in wet deposition ethanol concentration. Since 5 out of 8 outliers were of marine origin and 3 out of 8 outliers were of mixed origin, the data skewed significantly while including the outliers in the analysis. While excluding outliers, the VWA ethanol concentration influenced by marine and mixed sources changed from 3305 nM to 714 nM and 1688 nM to 759 nM respectively. So, the outliers were not included to examine the influence of airmass in VWA wet deposition ethanol concentration (Figure 11). The majority of airmasses originated from SE direction (54.17%) while no airmass originated from SW direction.

No significant difference in ethanol concentration according to airmass origin/ back trajectories was observed in this study (ANOVA, $\alpha = 0.05$, $n = 48$).

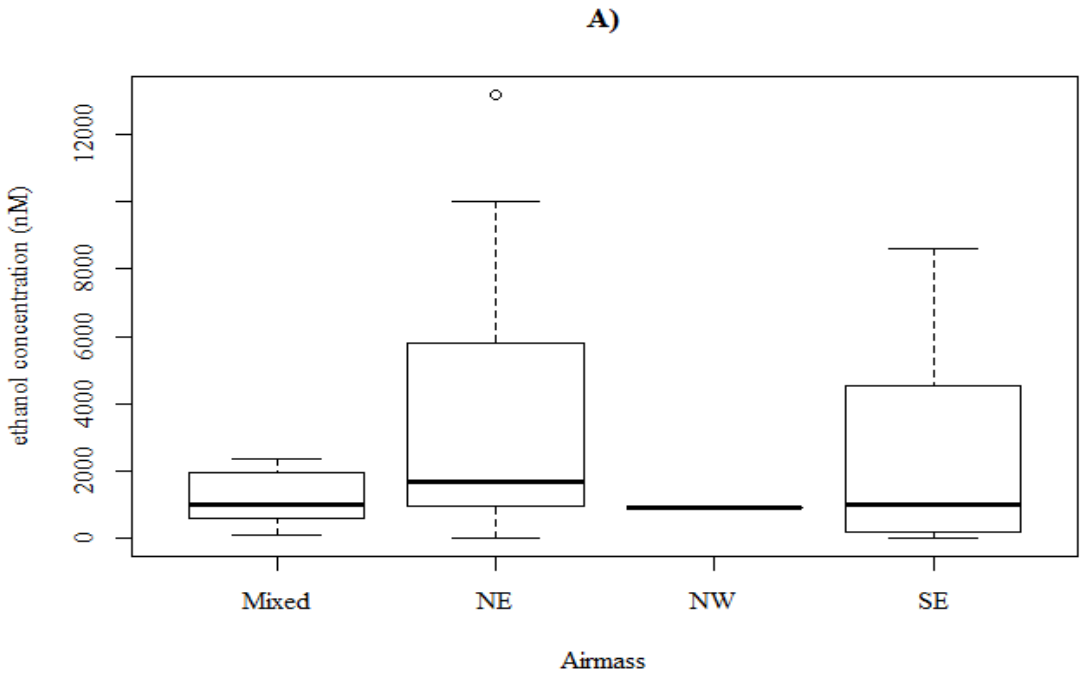

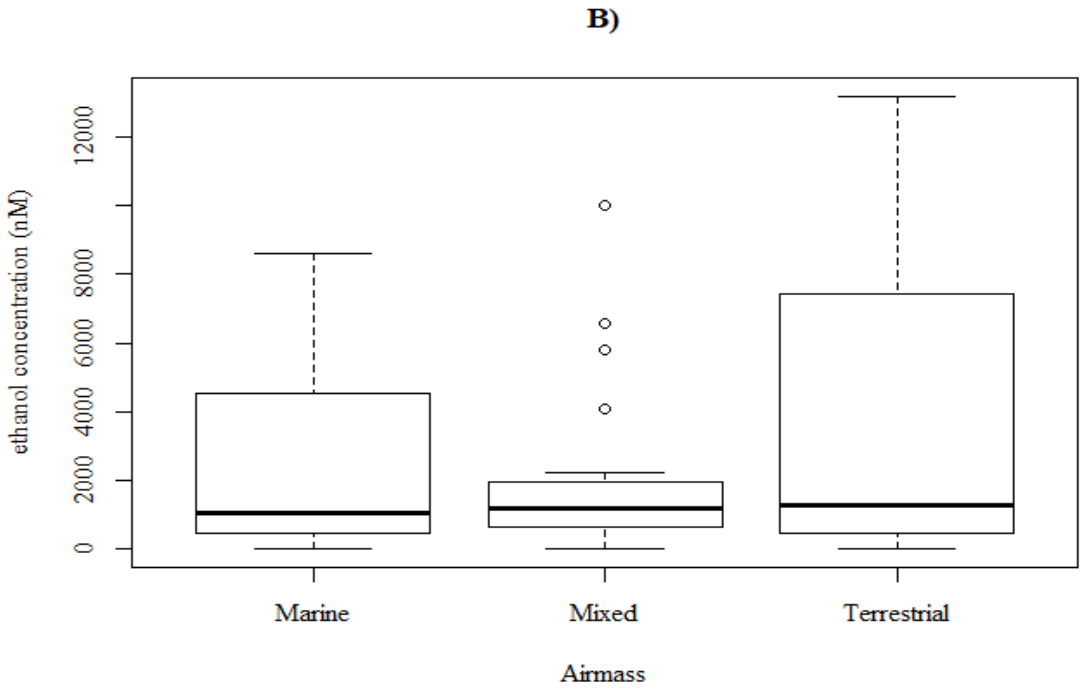

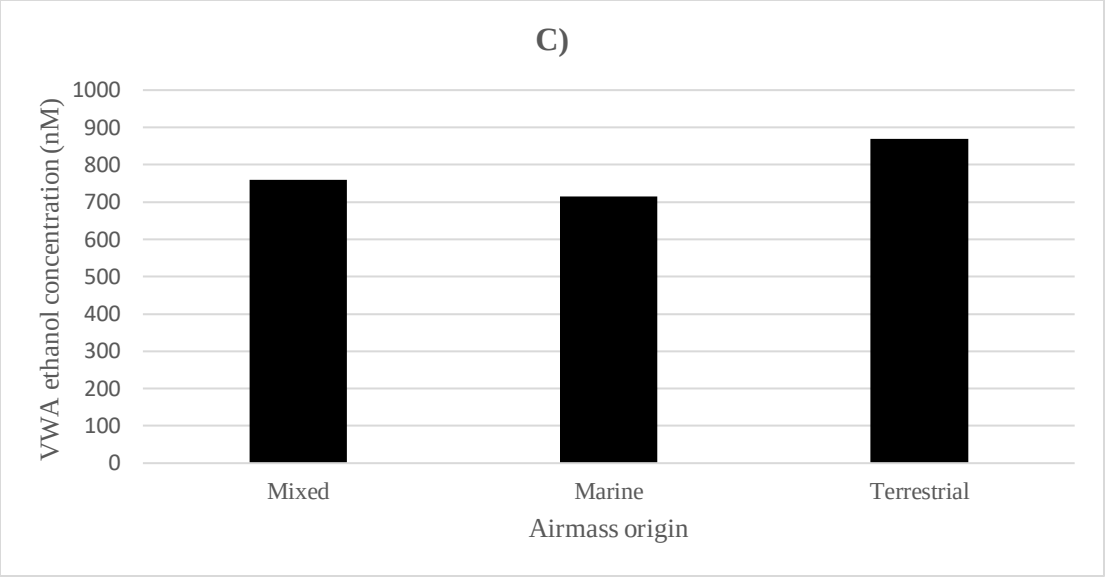

Figure 11. Variation of wet deposition ethanol according to airmass origin. Figure 11.A shows the box and whisker plot of the influence of airmass direction in wet deposition ethanol concentration, figure 11.B shows the box and whisker plot of the effect of terrestrial and marine sources in the ethanol concentration and figure 11.C shows the VWA ethanol concentration according to the airmass origin. Black horizontal dashed line inside the box represent the median, the box represents the interquartile range, the end bars represent the range and the circles represent the outliers in the figures 11.A and 11.B.While analyzing the VWA ethanol concentration vs airmass origin, outliers were not included as the data skewed significantly while including the outliers.

3.2.4 Ethanol concentration variation due to precipitation amount (TX)

The effect of precipitation amount for wet deposition ethanol concentration in Texas was also studied in this study to analyze how the analyte varied as a function of sample volume (Figure 12). Rainout effect was not observed in this study.

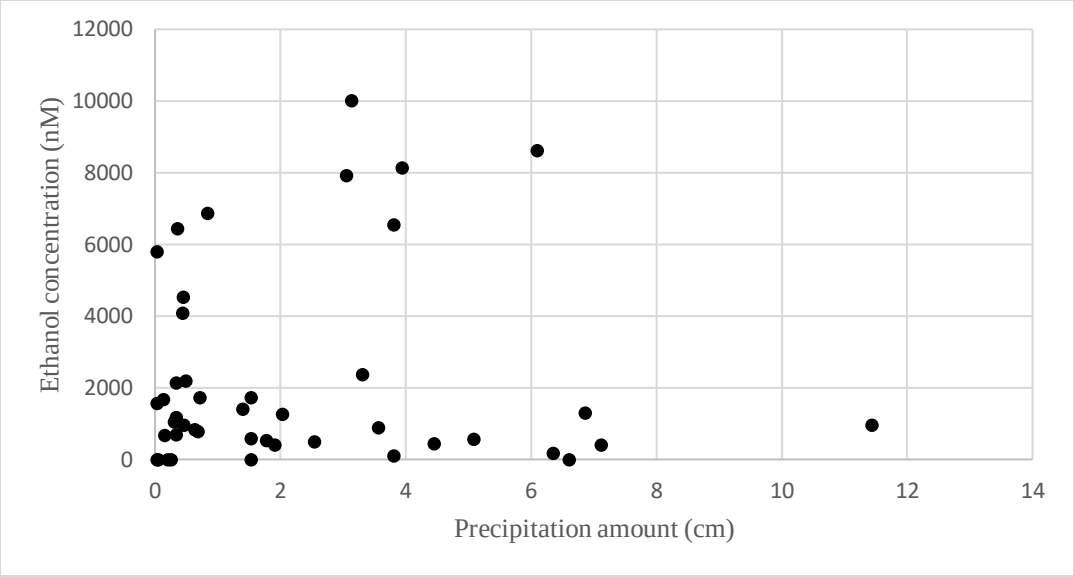

Figure 12. Ethanol concentration vs precipitation amount in all rain events in South Texas.

3.2.5 Intercorrelations (TX)

All ancillary rainwater components were analyzed by intercorrelation using Pearson correlation analysis. No significant correlation was observed between ethanol and any other components in the wet deposition (Table 4).

Table 4. Intercorrelation among ethanol, chloride, nitrate, sulfate, ammonium and hydrogen ion in wet deposition samples from South Texas site. Bold-faced values indicate significance at $p < 0.05$, $n = 12$

	Cl^-	NO_3^-	SO_4^{--}	NH_4^+	H^+
C_2H_5OH	0.09027	0.51241	0.32679	0.57562	0.10585
Cl^-		**0.04806**	**0.00002**	0.26473	**0.00004**
NO_3^-			0.19762	0.29484	0.26473
SO_4^{--}				0.47205	**0.00001**
NH_4^+					0.45245

3.3 Carbon isotopic composition of ethanol in wet deposition

The $\delta^{13}C$ values for wet deposition samples from Texas, TN00, WV99 and NY67 were -16.0 ± 0.6 (n = 3), -23.1 ± 0.3 (n = 3), -20.3 ± 0.7 (n = 1) and -17.0 ± 0.3 (n = 2) respectively. The anthropogenic endmember value of -9.8 ± 2.5‰ [*Felix et al.*, 2018] and biogenic endmember value of -30.9 ± 4.2‰ [*Giebel et al.*, 2011] were used to find the contribution from these sources, excluding the endmember values for C4 plants in the model (Table 5). Our results show that the anthropogenic source contribution was maximum in Texas out of all sites in the study. In AIRMoN sites, the maximum anthropogenic contribution to wet deposition ethanol was found in NY67 while the minimum anthropogenic contribution was found in TN00. At WV99, the contribution from anthropogenic and biogenic sources were almost equivalent.

Table 5. Anthropogenic and biogenic (excluding C4 plants) source contribution calculated by ISOERROR and SIAR.

Sites	ISOERROR		SIAR	
	Anthropogenic	Biogenic	Anthropogenic	Biogenic
Texas	70.6± 12.8%	29.4 ± 12.8%	68.4 ± 12.7%	31.6 ± 12.7%
TN00	36.8 ± 8.3%	63.2 ± 8.3%	39.6 ± 16.5%	60.4 ± 16.5%
WV99	50.4%	49.6%	47.8 ± 12.7%	52.2 ± 12.7%
NY67	66.1 ± 11.9%	33.9 ± 11.9%	63.4 ± 12.9%	36.6 ± 12.9%

The isotopic endmember value for C4 plants ($\delta^{13}C$ = -15.2 ± 0.5‰) was also included in the isotope mixing model equation to see the impacts in the source contribution [*Keppler et al.*, 2004]. The percentage contribution from biogenic and anthropogenic sources varied by a maximum of 20% while including C4 plants in the mixing model equation Compared to the

model that only included C3 plants (Table 7). The fraction of C3 and C4 plants shown in Table 6 was extracted from another independent study [*Still et al.*, 2003].

Table 6. Carbon isotopic end member value for biogenic sources in each site.

Sites	Fraction of C3 plants	Fraction of C4 plants	$\delta\ ^{13}C_{Ethanol}$ (Biogenic)
Texas	0.6	0.4	-24.6 ± 4.7‰
TN00	0.8	0.2	-27.7 ± 4.7‰
WV99	0.6	0.4	-24.6 ± 4.7‰
NY67	0.9	0.1	-29.3 ± 4.7‰
IL11	0.6	0.4	-24.6 ± 4.7‰
PA15	0.8	0.2	-27.7 ± 4.7‰

Table 7. Anthropogenic and biogenic (including C4 plants) source contribution calculated by ISOERROR and SIAR.

Sites	ISOERROR		SIAR	
	Anthropogenic	Biogenic	Anthropogenic	Biogenic
Texas	58.1 ± 14.8%	41.9 ± 14.8%	56.9 ± 16.0%	43.1 ± 16.0%
TN00	25.8 ± 10.1%	74.2 ± 10.1%	32.8 ± 18.3%	67.2 ± 18.3%
WV99	29.4%	70.7%	32.2 ± 14.8%	67.8 ± 14.8%
NY67	63.4 ± 12.6%	36.6 ± 12.6%	58.3 ± 19.5%	41.7 ± 19.5%

3.4 Global Wet Deposition Flux

The ethanol data from AIRMoN sites were added to the empirically-estimated global wet deposition flux dataset [*Felix et al.*, 2017] (Table 8). Out of five AIRMoN sites in this study,

PA15 site was the only site added to “Terrestrial with local source” group; all other four sites were added to “Terrestrial with no local source” group. The results show that the global wet deposition ethanol flux was 2.7 ± 1.3 Tg/yr. This average ethanol flux is in an agreement with previous models and estimates of global ethanol flux [*Naik et al.*, 2010]. However, this study is using data from 17 sites globally (out of which only 4 sites lie outside the US) to estimate the global wet deposition ethanol flux [*Felix et al.*, 2017]. Moreover, the wet deposition samples were not collected for all seasons due to lack of long-term sampling conditions which adds uncertainty to this wet deposition ethanol flux estimate.

Table 8. Global Wet Deposition Ethanol Flux calculated by separating wet deposition samples into "Terrestrial with no local source", "Terrestrial with local source" and “Marine source”. Preliminary data was also included from a literature [*Felix et al.*, 2017].

	Terrestrial – No Local Source	Terrestrial – Local Source	Marine Source
Ethanol Concentration, nM	365 ± 231	2053 ± 224	25 ± 6
Area of earth, m^2	$1.49 * 10^{14}$	$1.49 * 10^{14}$	$3.61 * 10^{14}$
Area of terrestrial classified as each	0.98	0.02	
Deposition amount, mm/yr	746	746	1066
Range of deposition rate of given category, Tg/yr	0.92 – 3.24	0.19 – 0.23	0.34 – 0.55
Global wet deposition rate, Tg/yr	**Minimum estimate**	**Mean estimate**	**Maximum estimate**
	1.5	2.7	4.0

4. DISCUSSION

4.1 AIRMoN

4.1.1 Wet deposition ethanol concentration

Out of 5 AIRMoN sites in the study, the VWA concentration of wet deposition ethanol is maximum in PA15 (1054.57 nM) (Figure 3). The airmass origin data indicates that the high ethanol concentration at PA15 might be coming from the NW direction (Appendix 2) where an ethanol production plant, that produces 110 million gallons of ethanol per year, is located ~48 km away [*Pennsylvania Grain Processing*, 2019]. All other AIRMoN sites showed a relatively lower (< 500 nM) VWA ethanol concentration except IL11 (687 nM). This high VWA ethanol concentration in IL11 is the result of 2 outliers (> 2000 nM) out of 10 samples. The outliers may be due to the emission from ethanol production plants as a significant amount of US ethanol (~12%) is produced in this state [*Nebraska Department of Environment and Energy*, 2019]. Out of all AIRMoN sites, the lowest wet deposition ethanol concentration was found in NY67. As NADP sites are meant to provide the regional data [*Bigelow et al.*, 2001] and the rain collection site in New York lies in a rural area, it is possible that this concentration represents typical background concentrations resulting from multiple regional sources.

4.1.2 Seasonal variation

All study sites showed no statistically significant seasonal variation in wet deposition ethanol concentration when studied individually or collectively (Figure 4, Figure 5). However, it was observed that the VWA ethanol concentration was minimum during summer and maximum during winter (Figure 5). As the season changes from winter to summer, the concentration of photochemically produced hydroxyl radical also increases in the atmosphere. This increased

hydroxyl radical leads to increased oxidation of ethanol to aldehydes, thus causing a decrease in wet deposition ethanol concentration from winter to summer. However, the concentration of hydroxyl radical begins to decrease after summer, thus decreasing the oxidation of ethanol and increasing the ethanol concentration in wet deposition [*Kieber et al.*, 2014]. Moreover, the maximum decomposition of dead and decayed organisms during fall also emits ethanol to the atmosphere [*Kirstine and Galbally*, 2012a].

4.1.3 Intercorrelations

No significant correlation ($p > 0.05$) was observed between wet deposition ethanol and any other analytes in most AIRMoN sites (Table 3, Appendices 4 – 8). The possible reason for this could be the different sources for ethanol and other analytes, or the difference in atmospheric residence time of ethanol and other analytes. The difference in the atmospheric residence time makes it difficult for all analytes emitting from a common source to get washed out at the same time during the wet deposition event because the analyte with shorter residence time could already leave the atmosphere before the wet deposition event. Also, there is a possibility that an airmass could cross some point sources of an analyte before reaching the wet deposition collection site, which will add the concentration of such analyte; thus, disrupting the correlation between wet deposition ethanol and the analyte.

A few significant correlations were observed at AIRMoN sites including correlations between ethanol and phosphate ion ($p = 0.0466$) at TN00 (Appendix 4) and ethanol and hydrogen ion concentration ($p = 0.0287$) at WV99 (Appendix 5). The phosphate in the atmosphere comes from anthropogenic activities like biomass burning, use of fertilizers or naturally from soil-derived dust [*Migon and Sandroni*, 1999]. The correlation between phosphate and cations like calcium, magnesium, potassium and sodium at TN00 indicates that the phosphate ion could be possibly

coming from dust particles [*Martins et al.*, 2019]. Since there is no correlation between ethanol and any other analytes except phosphate ion at TN00, it is difficult to pinpoint the possible reasons for this correlation. A significant correlation between ethanol and hydrogen ion concentration at WV99 could be possibly because the hydrogen ion was coming from organic acids like formate and acetate which are mostly biogenic [*Keene and Galloway*, 1984]. No significant correlations between hydrogen and sulfate or hydrogen and nitrate were observed, indicating that H^+ may not be linked to anthropogenic inputs [*Hu et al.*, 2003]. So, this correlation between ethanol and hydrogen could be the result of having a common biogenic source. When data from all AIRMoN sites were collectively analyzed, a significant correlation was found between ethanol and chloride and ethanol and sodium concentration (Table 2). One of the possible reasons for the significant correlation between ethanol and chloride might be because ethanol is primarily emitted from forested area and the fungal decomposition of woody material also emits methyl chloride to the atmosphere [*Khalil et al.*, 1999] in addition to ethanol. An ANOVA test ($\alpha = 0.05$) was also performed between ethanol concentration and chloride concentration in winter samples to determine whether the chloride ion was coming from road salts. However, no significant correlation was observed between winter ethanol and chloride concentration. The significant correlations ($p < 0.05$) of sodium and chloride with nitrate, sulfate and ammonium indicate the possibility of anthropogenic sources like livestock farming, cultivation or from industries [*Martins et al.*, 2019]. However, the airmass back-trajectories show that most of the airmasses are coming from mixed sources, indicating a possibility of long-range marine inputs. The ratio of [Cl-] to [Na+] in this study (1.22) was also similar to that of sea-salts (1.16) [*Hu et al.*, 2003]. Moreover, there was a strong correlation between [Cl-] and [Na+], indicating these ions could be of marine origin [*Song and Gao*, 2009]. Therefore, the correlation

of ethanol and sodium and ethanol and chloride could be possibly because of anthropogenic inputs or marine inputs. No correlations between ethanol and any other analytes were observed in this study. Moreover, there was no correlation between ethanol and precipitation amount in any sites when analyzed individually or collectively, similar to a recent study at Wilmington, North Carolina [*Kieber et al.,* 2014]. The possible reason for this is the continuous resupply of ethanol to the atmosphere, which suggests that ethanol was not completely washed out during the rain event [*Kieber et al.*, 2014].

4.1.4 Isotopic composition and source contribution

Two different approaches (including and excluding C4 plants) were used to determine the contribution of biogenic and anthropogenic sources to atmospheric ethanol. All studies to date have used the carbon isotopic endmember value of C3 plants as the endmember for biogenic sources because more than 95% of global plant biomass is comprised of C3 plants. However, in this study, we have also developed a mixing model that includes the carbon isotopic value of C4 plants in the biogenic endmember value to determine the difference in source contribution while including and excluding C4 plants. Also, two different models using frequentist (ISOERROR) and Bayesian statistics (SIAR) were used in both (including and excluding C4 plants) cases to see the difference based on models in each case.

The $\delta^{13}C$ values for wet deposition samples from TN00, WV99 and NY67 were -23.1 ± 0.3 (n = 3), -20.3 ± 0.7 (n = 1) and -17.0 ± 0.3 (n = 2) respectively. The less negative value for NY67 samples means a comparatively dominant anthropogenic source contribution in these sites. As New York is a state with the highest population density out of all AIRMoN site [*1keydata*, 2019], the high anthropogenic contribution in NY67 could possibly be from vehicular emissions.

The study also shows that while including C4 plants in models, the percent contribution from the biogenic/anthropogenic sources varied remarkably (by almost 20%) in comparison to the C3 plant model if the fraction of C4 plants in the state is high (like in the case of WV99 (~40%)). However, if the fraction of C4 plants is less (as in case of NY67 (~10%)), then the contribution varied only negligibly. Therefore, as the distribution of C3 and C4 plants varies from site to site, our study suggests that it is important to consider the types of plants around each site before assigning the representative endmember value for biogenic sources. However, it is currently unknown how the ethanol emission rates per C3 and C4 biomass vary and it should be the subject of future investigations. Moreover, the future studies should also include different types of C4 plants in their research to characterize the representative $\delta^{13}C$ value for a majority of C4 plants. This is because only one type of C4 plant (corn) has been analyzed so far compared to fifteen C3 plants [*Giebel et al.*, 2011, *Keppler et al.*, 2004].

4.2 TX

4.2.1 Wet deposition ethanol concentration

The volume weighted average concentration of wet deposition ethanol is maximum in Texas (1131 nM). This high concentration in Texas could be possibly from anthropogenic sources. Four ethane and ethylene cracking plants have been recently established in Texas that might have contributed for such a high concentration of wet deposition ethanol as ethanol is an oxidation product of ethane [*Doyle*, 2018]. The US EPA data shows that the production of ethane in the gulf coast region is increasing every year [*U.S. Energy Information Administration*, 2019a] and over half of the ethane (370 out of 623 million gallons) in the US is produced in this region every year [*U.S. Energy Information Administration*, 2019b]. Moreover, the rain collection site in Texas lies close (<100 m) to a moderately trafficked (27640 vehicles/day) four-lane road

[*Corpus Christi Metropolitan Planning Organization*, 2019]. This indicates that this data could be the result of ethanol emitted from vehicular exhaust.

Previous studies done in Wilmington, NC, USA show a lower wet deposition ethanol concentration for wet deposition with marine airmass origins [*Kieber et al.*, 2014; *Mullaugh et al.*, 2018]. However, no such difference in ethanol concentration according to airmass was observed in Texas in this study (ANOVA, $\alpha = 0.05$, P-value > 0.05). One of the possible reasons for this might be due to the presence of local sources. Even when an airmass primarily travels over a marine environment, it might pass through some point sources (e.g. distilleries) during transport to the wet deposition collection site which would cause the overall increase in the concentration of ethanol. The other possible reason might be the changing nature of coastal waters to act as a sink or source depending upon the ethanol concentration in overlying airmass [*Avery et al.*, 2016]. The ethanol concentration in the overlying airmass relies upon factors affecting air-sea flux exchange like temperature and aqueous concentration as well as biological and photochemical conditions [*Beale et al.*, 2010].

4.2.2 Seasonal Variation

It was observed that the concentration of wet deposition ethanol was higher in fall and winter in Texas in comparison to that in summer and spring. However, no significant variation in ethanol concentration according to seasons was observed. The higher concentration in fall and winter could be from increased ethanol emission by microbial activities on dead and decaying biomass during this time of the year [*Karl et al.*, 2003]. Also, the decrease in the loss of atmospheric ethanol by photo-oxidation during fall and winter might have resulted in relatively higher concentration of wet deposition ethanol during these seasons as the solar irradiance is the lowest during this time of the year [*Mullaugh et al.*, 2018].

4.2.3 Intercorrelations

No significant correlation was observed between wet deposition ethanol and any other analytes in South Texas (Table 3, Appendices 4 – 8). The possible reason for this could be the different sources for ethanol and other analytes, or the difference in atmospheric residence time of ethanol and other analytes. The difference in the atmospheric residence time makes it difficult for all analytes emitting from a common source to get washed out at a same time during the wet deposition event because the analyte with shorter residence time could already leave the atmosphere before the wet deposition event. Also, there is a possibility that an airmass could cross some point sources of an analyte before reaching the wet deposition collection site, which will add the concentration of such analyte; thus, disrupting the correlation between wet deposition ethanol and the analyte.

4.2.4 Isotopic composition and source contribution

The $\delta^{13}C$ values for wet deposition samples from Texas was -16.0 ± 0.6‰ (n = 3) which means there is a relatively dominant anthropogenic source contribution than the biogenic source. The high anthropogenic contribution in Texas could be possibly because of ethanol emissions from vehicles. Unlike AIRMoN sites, that are located in rural area to give regional representation [*Bigelow et al.*, 2001], the rain collection site in Texas lies close to a four-lane road in a densely populated urban area where the average number of traffic per day is 27640 [*Corpus Christi Metropolitan Planning Organization*, 2019].

5. CONCLUSION AND IMPLICATIONS

This study provides the first detailed temporal study of wet deposition ethanol representing a large area of the Eastern US and South Texas. Collection sites near ethanol producing factories and ethane and ethylene cracking plants showed a higher wet deposition ethanol concentration than the sites lacking such local sources, indicating that the impact of such local inputs can be clearly detected in wet deposition. Thus, an increase in the number of ethanol production plants will also increase in the concentration of ethanol in the atmosphere. The global wet deposition flux estimate lies within the range of previous estimates, implying that the wet deposition ethanol is near to the equilibrium with atmospheric ethanol. This means that when the concentration of atmospheric ethanol increases, the wet deposition removal should also increase to maintain the equilibrium between ethanol in wet deposition and atmospheric ethanol.

Ethanol reacts with hydroxyl radical in the atmosphere, thus increasing atmospheric ethanol concentration will have a significant impact in the oxidizing capacity of the atmosphere. Results of this study are important as it provides atmospheric scientists, environmental chemists and policy makers with a baseline of atmospheric ethanol concentration in order to help determine the efficacy of future ethanol fuel use and to help quantify the wet deposition ethanol sink. As this study also shows the change in source contribution while including C4 plants signature in the model, it suggests future researchers to incorporate the types of plants around the collection sites to determine the representative isotopic endmember value for biogenic sources. However, as the ethanol emission rate per C3 and C4 plants is currently unknown, this should be the subject of future investigation. Moreover, the future studies should further characterize the representative $\delta^{13}C$ value for a majority of C4 plants.

REFERENCES

1keydata (2019), List of States by Population Density, edited Retrieved from https://state.1keydata.com/state-population-density.php

American Association for the Advancement of Science (2019), AAAS Atlas of population and environment, edited Retrieved from http://atlas.aaas.org/

Avery, G. B., Jr., et al. (2016), Surface waters as a sink and source of atmospheric gas phase ethanol, *Chemosphere*, *144*, 360-365.

Avery Jr, G. B., R. J. Kieber, M. Witt, and J. D. Willey (2006), Rainwater monocarboxylic and dicarboxylic acid concentrations in southeastern North Carolina, USA, as a function of air-mass back-trajectory, *Atmospheric Environment*, *40*(9), 1683-1693.

Beale, R., P. S. Liss, and P. D. Nightingale (2010), First oceanic measurements of ethanol and propanol, *Geophysical Research Letters*, *37*(24).

Bigelow, D. S., S. R. Dossett, and V. C. Bowersox (2001), *Instruction manual: NADP/NTN site selection and installation*, NADP Program Office, Illinois State Water Survey.

Coplen, T. B., W. A. Brand, M. Gehre, M. Gröning, H. A. Meijer, B. Toman, and R. M. Verkouteren (2006), New guidelines for δ 13C measurements, *Analytical chemistry*, *78*(7), 2439-2441.

Copolovici, L., and Ü. Niinemets (2010), Flooding induced emissions of volatile signalling compounds in three tree species with differing waterlogging tolerance, *Plant, cell & environment*, *33*(9), 1582-1594.

Corpus Christi Metropolitan Planning Organization (2019), Traffic Count Portal, edited Retrieved from http://www.corpuschristi-mpo.org/07_gis_tcportal.html

Doyle, H. (2018), US chemical capacity to increase by more than 50 million tonnes, edited Retrieved from http://analysis.petchem-update.com/engineering-and-construction/us-chemical-capacity-increase-more-50-million-tonnes

Felix, J. D., R. Thomas, M. Casas, M. S. Shimizu, G. B. Avery, R. J. Kieber, R. N. Mead, C. S. Lane, J. D. Willey, and A. Guy (2018), Compound-Specific Carbon Isotopic Composition of Ethanol in Brazil and US Vehicle Emissions and Wet Deposition, *Environmental science & technology*.

Felix, J. D., et al. (2017), Removal of atmospheric ethanol by wet deposition, *Global Biogeochemical Cycles*.

Fukui, Y., and P. V. Doskey (1998), Air-surface exchange of nonmethane organic compounds at a grassland site: Seasonal variations and stressed emissions, *Journal of Geophysical Research: Atmospheres*, *103*(D11), 13153-13168.

Giebel, B. M., P. K. Swart, and D. D. Riemer (2011), New insights to the use of ethanol in automotive fuels: a stable isotopic tracer for fossil- and bio-fuel combustion inputs to the atmosphere, *Environmental science & technology*, *45*(15), 6661-6669.

Goldemberg, J., F. F. Mello, C. E. Cerri, C. A. Davies, and C. C. Cerri (2014), Meeting the global demand for biofuels in 2021 through sustainable land use change policy, *Energy Policy*, *69*, 14-18.

Guenther, A., C. N. Hewitt, D. Erickson, R. Fall, C. Geron, T. Graedel, P. Harley, L. Klinger, M. Lerdau, and W. McKay (1995), A global model of natural volatile organic compound emissions, *Journal of Geophysical Research: Atmospheres*, *100*(D5), 8873-8892.

Guy, A. L. (2013), Development of Method for Ethanol Extraction from Environmental Sources Using Solid-phase Microextraction to Determine Sources, University of North Carolina Wilmington.

Guyon, I., A. Saffari, G. Dror, and G. Cawley (2010), Model selection: Beyond the bayesian/frequentist divide, *Journal of Machine Learning Research*, *11*(Jan), 61-87.

Hoefs, J., and J. Hoefs (1997), *Stable isotope geochemistry*, Springer.

Holmes, R. M., A. Aminot, R. Kérouel, B. A. Hooker, and B. J. Peterson (1999), A simple and precise method for measuring ammonium in marine and freshwater ecosystems, *Canadian Journal of Fisheries and Aquatic Sciences*, *56*(10), 1801-1808.

Hu, G., R. Balasubramanian, and C. Wu (2003), Chemical characterization of rainwater at Singapore, *Chemosphere*, *51*(8), 747-755.

Jardine, K. J., E. D. Sommer, S. R. Saleska, T. E. Huxman, P. C. Harley, and L. Abrell (2010), Gas phase measurements of pyruvic acid and its volatile metabolites, *Environmental science & technology*, *44*(7), 2454-2460.

Karl, T., A. Guenther, C. Spirig, A. Hansel, and R. Fall (2003), Seasonal variation of biogenic VOC emissions above a mixed hardwood forest in northern Michigan, *Geophysical Research Letters*, *30*(23).

Keene, W. C., and J. N. Galloway (1984), Organic acidity in precipitation of North America, *Atmospheric Environment (1967)*, *18*(11), 2491-2497.

Keppler, F., R. Kalin, D. Harper, W. McRoberts, and J. Hamilton (2004), Carbon isotope anomaly in the major plant C 1 pool and its global biogeochemical implications, *Biogeosciences*, *1*(2), 123-131.

Khalil, M. A. K., R. M. Moore, J. M. Lobert, and W. T. Sturges (1999), Natural emissions of chlorine-containing gases, *Journal of Geophysical Research*, *104*(D7), 8333-8346.

Kieber, R. J., S. Tatum, J. D. Willey, G. B. Avery, and R. N. Mead (2014), Variability of ethanol and acetaldehyde concentrations in rainwater, *Atmospheric Environment*, *84*, 172-177.

Kieber, R. J., A. L. Guy, J. A. Roebuck, A. L. Carroll, R. N. Mead, S. B. Jones, F. F. Giubbina, M. L. Campos, J. D. Willey, and G. B. Avery (2013), Determination of ambient ethanol concentrations in aqueous environmental matrixes by two independent analyses, *Analytical chemistry*, *85*(12), 6095-6099.

Kirstine, W. V., and I. E. Galbally (2012a), Ethanol in the Environment: A Critical Review of Its Roles as a Natural Product, a Biofuel, and a Potential Environmental Pollutant, *Critical Reviews in Environmental Science and Technology*, *42*(16), 1735-1779.

Kirstine, W. V., and I. E. Galbally (2012b), The global atmospheric budget of ethanol revisited, *Atmospheric Chemistry and Physics*, *12*(1), 545-555.

MacDonald, R. C., T. W. Kimmerer, and M. Razzaghi (1989), Aerobic ethanol production by leaves: evidence for air pollution stress in trees of the Ohio River Valley, USA, *Environmental Pollution*, *62*(4), 337-351.

Manter, D. K., and R. G. Kelsey (2008), Ethanol accumulation in drought-stressed conifer seedlings, *International journal of plant sciences*, *169*(3), 361-369.

Martins, E. H., D. C. Nogarotto, J. Mortatti, and S. A. Pozza (2019), Chemical composition of rainwater in an urban area of the southeast of Brazil, *Atmospheric Pollution Research*, *10*(2), 520-530.

Migon, C., and V. Sandroni (1999), Phosphorus in rainwater: Partitioning inputs and impact on the surface coastal ocean, *Limnology and Oceanography*, *44*(4), 1160-1165.

Millet, D. B., E. Apel, D. K. Henze, J. Hill, J. D. Marshall, H. B. Singh, and C. W. Tessum (2012), Natural and anthropogenic ethanol sources in North America and potential atmospheric impacts of ethanol fuel use, *Environmental science & technology*, *46*(15), 8484-8492.

Millet, D. B., A. Guenther, D. A. Siegel, N. B. Nelson, H. B. Singh, J. A. de Gouw, C. Warneke, J. Williams, G. Eerdekens, and V. Sinha (2010), Global atmospheric budget of acetaldehyde: 3-D model analysis and constraints from in-situ and satellite observations, *Atmospheric Chemistry and Physics*, *10*(7), 3405-3425.

Mullaugh, K. M., M. S. Shimizu, J. D. Willey, J. D. Felix, R. J. Kieber, G. B. Avery Jr, R. N. Mead, C. Andreacchi, and A. Payne (2018), Variability of ethanol concentration in rainwater driven by origin versus season in coastal and inland North Carolina, USA, *Chemosphere*, *195*, 793-799.

NADP (2018), *Atmospheric Integrated Research Monitoring Network Site Operations Manual*.

Naik, V., A. M. Fiore, L. W. Horowitz, H. B. Singh, C. Wiedinmyer, A. Guenther, J. A. de Gouw, D. B. Millet, P. D. Goldan, and W. C. Kuster (2010), Observational constraints on the global atmospheric budget of ethanol, *Atmospheric Chemistry and Physics*, *10*(12), 5361-5370.

National Oceanic and Atmospheric Administration (2018), HYSPLIT Trajectory Model, edited Retrieved from https://www.ready.noaa.gov/hypub-bin/trajtype.pl?runtype=archive

Nebraska Department of Environment and Energy (2019), Ethanol Failities' Capacity by State, edited Retrieved from http://www.neo.ne.gov/programs/stats/inf/121.htm

Peixoto, J. P., and A. H. Oort (1992), *Physics of climate*, 172 pp.

Pennsylvania Grain Processing, L. (2019), Pennsylvania Grain Processing: A Producer of Ethaanol and DDGS, edited Retrieved from https://www.pagrain.com/

Phillips, D. L., and J. W. Gregg (2001), Uncertainty in source partitioning using stable isotopes, *Oecologia*, *127*(2), 171-179.

Poulopoulos, S., D. Samaras, and C. Philippopoulos (2001), Regulated and unregulated emissions from an internal combustion engine operating on ethanol-containing fuels, *Atmospheric environment*, *35*(26), 4399-4406.

Renewable Fuels Association (2018), Annual U.S. Fuel Ethanol Production, edited Retrieved from https://ethanolrfa.org/resources/industry/statistics/#1537811482060-17cad4ed-d2ca

Salvo, A., and F. M. Geiger (2014), Reduction in local ozone levels in urban São Paulo due to a shift from ethanol to gasoline use, *Nature Geoscience*, *7*(6), 450.

Sharp, Z. (2017), Principles of stable isotope geochemistry.

Singh, H., L. Salas, R. Chatfield, E. Czech, A. Fried, J. Walega, M. Evans, B. Field, D. Jacob, and D. Blake (2004), Analysis of the atmospheric distribution, sources, and sinks of oxygenated volatile organic chemicals based on measurements over the Pacific during TRACE-P, *Journal of Geophysical Research: Atmospheres*, *109*(D15).

Song, F., and Y. Gao (2009), Chemical characteristics of precipitation at metropolitan Newark in the US East Coast, *Atmospheric Environment*, *43*(32), 4903-4913.

Still, C. J., J. A. Berry, G. J. Collatz, and R. S. DeFries (2003), Global distribution of C3 and C4 vegetation: carbon cycle implications, *Global Biogeochemical Cycles*, *17*(1), 6-1-6-14.

U.S. Energy Information Administration (2016), U.S. Production, Consumption, and Trade of Ethanol, edited Retrieved from https://www.afdc.energy.gov/data/10323

U.S. Energy Information Administration (2019a), Gulf Coast (PADD 3) Field Production of Ethane, edited Retrieved from

https://www.eia.gov/dnav/pet/hist/LeafHandler.ashx?n=PET&s=M_EPLLEA_FPF_R30_MBBL&f=A

U.S. Energy Information Administration (2019b), Supply and Deposition, edited Retrieved from https://www.eia.gov/dnav/pet/pet_sum_snd_a_EPLLEA_mbbl_a_cur.htm

United States Census Bureau, U. D. o. C. (2016), edited Retrieved from https://www2.census.gov/geo/docs/maps-data/data/gazetteer/2016_Gazetteer/2016_gaz_place_17.txt

US Climate Data (2018a), Corpus Christi Weather Averages, edited, US Climate Data Retrieved from https://www.usclimatedata.com/climate/corpus-christi/texas/united-states/ustx0294

US Climate Data (2018b), Ithaca Weather Averages, edited Retrieved from https://www.usclimatedata.com/climate/ithaca/new-york/united-states/usny0717

US Climate Data (2018c), State College Weather Average, edited Retrieved from https://www.usclimatedata.com/climate/state-college/pennsylvania/united-states/uspa2543

US Climate Data (2018d), Oak Ridge Weather Averages, edited Retrieved from https://www.usclimatedata.com/climate/oak-ridge/tennessee/united-states/ustn0370

US Climate Data (2018e), Davis Weather Averages, edited Retrieved from https://www.usclimatedata.com/climate/davis/west-virginia/united-states/uswv0976

US Department of Commerce (2010), 2010 United States Census, edited

US Department of Energy (2018), Alternative Fuels Data Center, edited Retrieved from https://www.afdc.energy.gov/fuels/ethanol.html

Willey, J. D., G. B. Avery, J. D. Felix, R. J. Kieber, R. N. Mead, and M. S. Shimizu (2019), Rapidly increasing ethanol concentrations in rainwater and air, *npj Climate and Atmospheric Science*, *2*(1), 3.

World Media Group (2018a), Bondville,IL Weather, edited Retrieved from http://www.usa.com/bondville-il-weather.htm

World Media Group (2018b), West Virginia Average Precipitation City Rank, edited Retrieved from http://www.usa.com/rank/west-virginia-state--average-precipitation--city-rank.htm?hl=Davis&hlst=WV

APPENDICES

Appendix 1. Seasonal variation of VWA ethanol concentration in individual AIRMoN sites

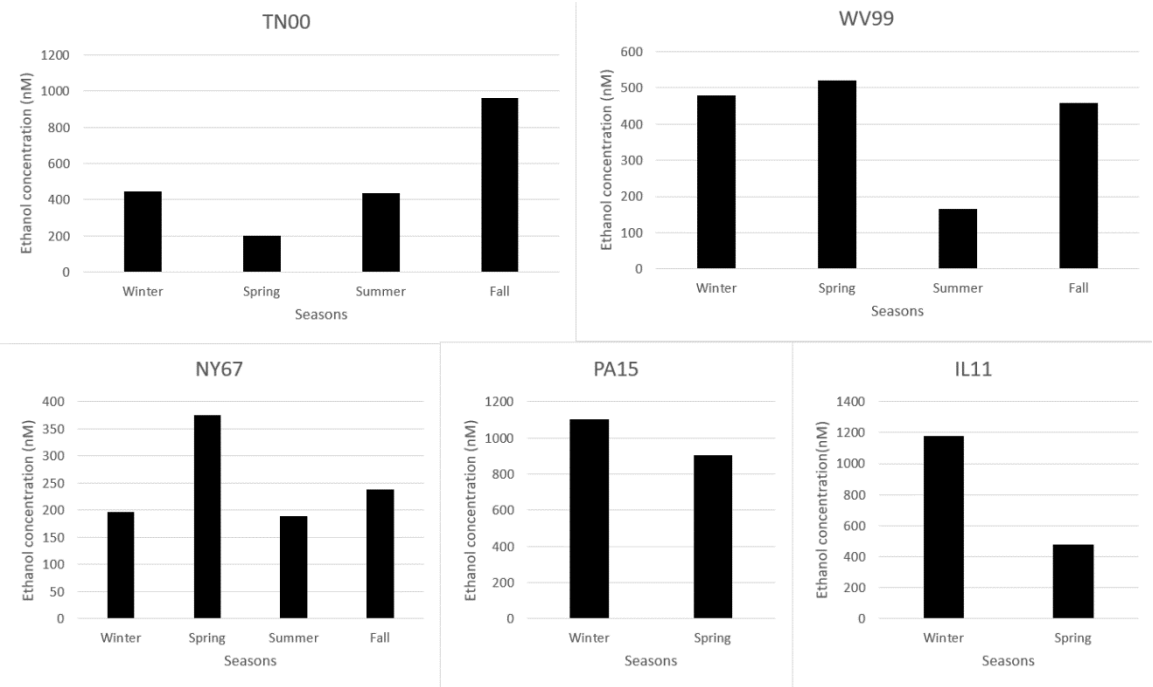

Appendix 2. Percentage of airmass origin in AIRMoN sites

Airmass / AIRMoN Sites	NW (%)	NE (%)	SE (%)	SW (%)	Mixed (%)
TN00	22.73	2.27	25	20.45	29.55
WV99	30.36	5.36	3.57	30.36	30.36
NY67	32.89	7.89	7.89	14.47	36.84
PA15	37.5	12.5	0	18.75	31.25
IL11	30	10	10	10	40

Appendix 3. Ethanol concentration vs precipitation amount in individual AIRMoN sites

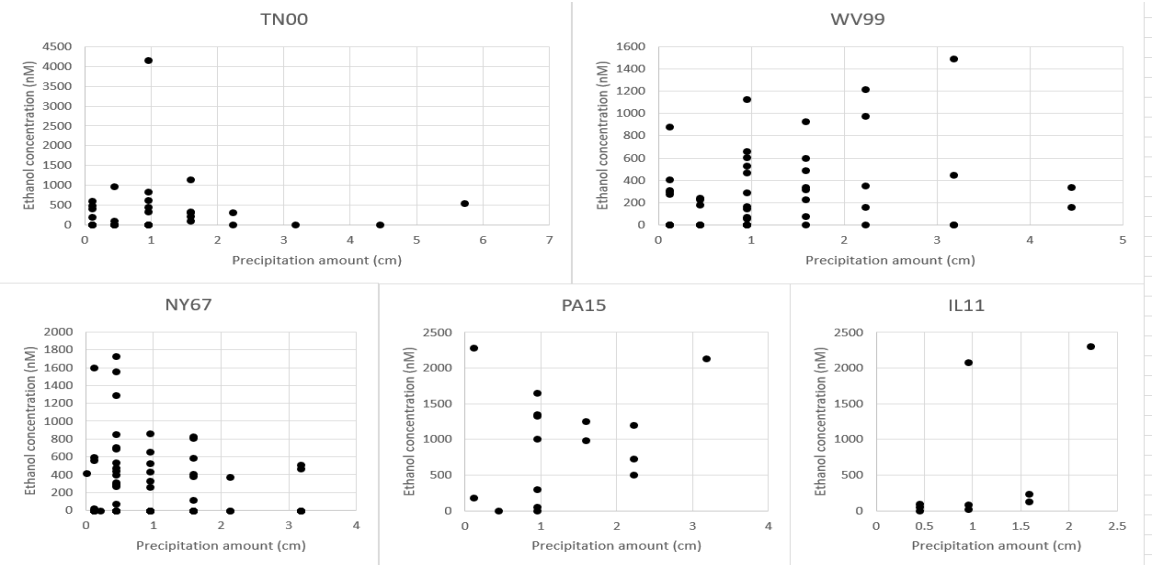

Appendix 4. Intercorrelation among ethanol, chloride, nitrate, sulfate, ammonium and hydrogen ion in wet deposition samples of TN00. Bold-faced values indicate significance at $p < 0.05$, n = 24

	Cl^-	NO_3^-	SO_4^{--}	NH_4^+	H^+	Ca^{++}	Mg^{++}	K^+	Na^+	PO_4^{---}
C_2H_5OH	0.1153	0.3739	0.4842	0.9630	0.2387	0.9621	0.3378	0.3137	0.1404	**0.0466**
Cl^-		**0.01285**	**0.0019**	**0.0054**	0.9963	0.1693	**<0.0001**	**< 0.0001**	**< 0.0001**	**0.0151**
NO_3^-			**< 0.0001**	**< 0.0001**	**0.0019**	**0.1274**	**0.0054**	0.0840	**0.0151**	0.3247
SO_4^{--}				**< 0.0001**	0.1274	**0.0360**	**0.0016**	**0.0176**	**0.0054**	0.0596
NH_4^+					0.0596	**0.0360**	**0.0003**	**0.0065**	**0.0054**	**0.0360**
H^+						0.1544	0.9630	0.1153	0.9630	0.0528
Ca^{++}							**< 0.0001**	**0.0044**	0.0528	**0.0012**
Mg^{++}								**< 0.0001**	**< 0.0001**	**< 0.0001**
K^+									**< 0.0001**	**< 0.0001**
Na^+										**0.0008**

Appendix 5. Intercorrelation among ethanol, chloride, nitrate, sulfate, ammonium and hydrogen ion in wet deposition samples of WV99. Bold-faced values indicate significance at $p < 0.05$, n = 35

	Cl^-	NO_3^-	SO_4^{--}	NH_4^+	H^+	Ca^{++}	Mg^{++}	K^+	Na^+	PO_4^{---}
C_2H_5OH	0.0780	0.2743	0.1838	0.1024	**0.0287**	0.0699	0.0800	0.9545	0.9545	0.2494
Cl^-		**<0.0001**	**0.0067**	**0.0002**	0.9955	0.9092	0.9545	0.9092	**0.0393**	0.9545
NO_3^-			**<0.0001**	**<0.0001**	0.9909	0.5676	0.7755	0.9545	0.6478	0.9092
SO_4^{--}				**<0.0001**	0.0529	0.1838	0.2260	0.0910	0.1167	0.2260
NH_4^+					0.0800	0.3289	0.7755	0.1475	0.1167	0.6071
H^+						0.9545	0.9545	0.8642	0.9092	0.9636
Ca^{++}							**<0.0001**	**<0.0001**	**0.0002**	**<0.0001**
Mg^{++}								**<0.0001**	**< 0.0001**	**<0.0001**
K^+									**0.0022**	**<0.0001**
Na^+										0.0529

Appendix 6. Intercorrelation among ethanol, chloride, nitrate, sulfate, ammonium and hydrogen ion in wet deposition samples of NY67. Bold-faced values indicate significance at $p < 0.05$, n = 34

	Cl^-	NO_3^-	SO_4^{--}	NH_4^+	H^+	Ca^{++}	Mg^{++}	K^+	Na^+	PO_4^{---}
C_2H_5OH	0.9996	0.9996	0.9552	0.9996	0.1539	0.9552	0.9106	0.0847	0.9776	0.9106
Cl^-		**0.0041**	0.0744	0.2112	0.9996	0.0961	**0.0021**	0.9106	**<0.0001**	0.0961
NO_3^-			**<0.0001**	**<0.0001**	0.3084	**0.0134**	**0.0033**	0.2332	0.0744	**0.0134**
SO_4^{--}				**<0.0001**	0.9996	**0.0002**	**0.0001**	**0.0001**	0.2332	**0.0002**
NH_4^+					0.2568	**0.0008**	**0.0010**	**0.0001**	0.9552	**0.0008**
H^+						**0.0491**	0.0961	0.0566	0.9106	**0.0491**
Ca^{++}							**<0.0001**	**<0.0001**	0.065	**<0.0001**
Mg^{++}								**<0.0001**	**0.0004**	**<0.0001**
K^+									0.0744	**<0.0001**
Na^+										0.0650

Appendix 7. Intercorrelation among ethanol, chloride, nitrate, sulfate, ammonium and hydrogen ion in wet deposition samples of PA15. Bold-faced values indicate significance at $p < 0.05$, n = 14

	Cl^-	NO_3^-	SO_4^{--}	NH_4^+	H^+	Ca^{++}	Mg^{++}	K^+	Na^+	PO_4^{---}
C_2H_5OH	0.2492	0.6331	0.3693	0.9973	0.5848	0.9973	0.9973	0.7857	0.2492	0.9729
Cl^-		0.1802	0.0566	0.9729	**0.0264**	0.7338	**0.0013**	0.0753	**<0.0001**	0.9729
NO_3^-			0.0979	**0.0233**	0.2647	0.0687	**0.0264**	**0.0044**	0.1802	**0.0063**
SO_4^{--}				**0.0333**	0.5381	**0.0037**	**0.0157**	**0.0233**	0.1929	0.1929
NH_4^+					0.1154	**0.0075**	0.0566	**0.0010**	0.9729	**0.0010**
H^+						0.3887	0.9459	0.9729	0.1249	0.9729
Ca^{++}							**0.0205**	**0.0030**	0.3323	0.3505
Mg^{++}								**<0.0001**	**<0.0001**	0.1154
K^+									**0.0180**	**0.0075**
Na^+										0.9729

Appendix 8. Intercorrelation among ethanol, chloride, nitrate, sulfate, ammonium and hydrogen ion in wet deposition samples of IL11. Bold-faced values indicate significance at $p < 0.05$, n = 6

	Cl^-	NO_3^-	SO_4^{--}	NH_4^+	H^+	Ca^{++}	Mg^{++}	K^+	Na^+	PO_4^{---}
C_2H_5OH	.3587	.6328	.7329	.5499	.9850	0.5097	0.3125	0.1372	0.5097	0.1140
Cl^-		.3826	.2276	.4320	0.1711	0.1454	**0.0364**	**0.0321**	**0.0006**	**0.0364**
NO_3^-			**0.0243**	0.4070	0.3469	**0.0053**	**0.0409**	0.1215	0.4574	0.1454
SO_4^{--}				0.6048	0.3826	**0.0024**	**0.0175**	0.0733	0.2276	0.1066
NH_4^+					0.2903	0.6048	0.9850	0.9700	0.3826	0.9700
H^+						0.3238	0.2478	0.4833	0.2376	0.5364
Ca^{++}							**0.0024**	**0.0242**	0.1623	**0.0364**
Mg^{++}								**0.0037**	0.0560	**0.0072**
K^+									0.0507	**<0.0001**
Na^+										0.0560